Molecular Characterization of the Binding Site of Nematode $GABA_A$ Receptors

By

Michael V. Accardi

A Thesis Submitted in Partial Fulfillment

Of the Requirements for the Degree of

Masters of Science

In

The Faculty of Science

Applied Bioscience

University of Ontario Institute of Technology

August, 2010

Certification of Approval

Copyright Agreement

Abstract

Haemonchus contortus is a parasitic nematode that is controlled in large part by nematocidal drugs that target receptors of the parasitic nervous system. Hco-UNC-49 is a nematode GABA receptor that has a relatively low overall sequence homology to mammalian GABA receptors but is very similar to the UNC-49 receptor found in the free living nematode *Caenorhabditis elegans*. However, the nematode receptors do exhibit different sensitivities to GABA which may be linked to differences in the putative GABA binding domains. Mutational analysis conducted in this study identified at least one amino acid, positioned near the GABA binding domain, which may partially account for differences in nematode GABA sensitivity. In addition, positions reported to be crucial for GABA sensitivity in mammalian receptors also affect GABA sensitivity in Hco-UNC-49 suggesting that the GABA binding domains of the mammalian and nematode GABA receptors share some pharmacological similarities. However, there were some differences observed. For example, in mammalian $GABA_A$ receptors amino acids from both β and α subunits appear to be important for GABA sensitivity. For residues examined in this study, only those on the UNC-49B subunit, and not UNC-49C, appear important for GABA sensitivity.

KEYWORDS

Haemonchus contortus, GABA, ligand binding, mutational analysis, homology modelling

Acknowledgments

I would personally like to thank my supervisor Dr. Sean Forrester for all his patience and guidance throughout my graduate studies. Without Dr. Forrester's assistance during this investigation, I sincerely feel that I would not have matured as much as I have as a researcher and thinker. I would also like to thank the whole Forrester Lab, both past and present. Your ability to make me laugh, enter into discussions ranging from the biggest science questions to the most immature anecdote, and our alliances in Risk (Go Team Forrester!) have made my Master's one of the most enjoyable experiences of my life. I would also like to extend my appreciation towards the University of Ontario Institute of Technology, specifically the Faculty of Science, for this great opportunity. I've enjoyed watching and being part of the university's growth and wish you all the best in the future.

Finally, I would like to acknowledge and thank my family, friends and that special someone (you know who you are). Without your endless support and encouragement this Master's would not have been possible.

Table of Contents

List of Tables

List of Figures

List of Appendices

List of Abbreviations

5-HT_3	Serotonin-gated cation channels
AChBP	Acetylcholine binding protein
Ala	Alanine
Arg	Arginine
ben-1	Benzimidazole resistant mutant
BDI	Binding domain I
BDII	Binding domain II
cDNA	Complementary DNA
Cel-UNC-49	*Caenorhabditis elegans* uncoordinated gene 49
CNS	Central nervous system
cRNA	copy ribonucleic acid
Cys-loop	Cysteine-loop
DALY	Disability adjusted life year
DD	Dorsal D-type motor neuron
DNA	Deoxyribonucleic acid
EC_{50}	Half-maximal channel activity
GABA	γ-aminobutyric acid
Grd	*Glycine-like receptor* of Drosophila
Hco-LGC-38	*Haemonchus contortus* RDL homologue
Hco-UNC-49	*Haemonchus contortus* uncoordinated gene 49
IVM	Ivermectin
KCL	Potassium chloride
L1-L4	Larval growth stage 1 - 4
Lcch3	*Ligand-gated chloride channel homologue 3*
Leu	Leucine

LGCC	Ligand-gated chloride channels
LGIC	Ligand-gated ion channels
Met	Methionine
MS-222	Ethyl 3-amino benzoate methane sulfonate
nAChRs	Nicotinic acetylcholine receptors
Phe	Phenylalanine
PTX	Picrotoxin
Rdl	Resistance to dieldrin-like
RNA	Ribonucleic acid
Ser	Serine
SSU rRNA	Small subunit ribosomal RNA
tub-1	*H. contortus* isotype 1 β-tubulin gene
TM1-TM4	Transmembrane domains 1 – 4
Thr	Threonine
Tyr	Tyrosine
unc	Uncoordinated genes
VD	Ventral D-type motor neuron
VGAT	Vesicular GABA transporter

Chapter 1 – Introduction

1.1 The Phylum Nematoda

The phylum Nematoda (roundworms) represents one of the most diverse groups of organisms found on the planet (Gilleard, 2004; Nikolaou and Gasser, 2006). Estimates suggest that nematodes encompasses roughly 100,000 to 1 million extant species exploiting a wide variety of niches include free living, terrestrial and marine microbivores, meiofaunal predators, herbivores, and plant and animal parasites (Parkinson *et al.* 2004). Small subunit ribosomal ribonucleic acid (SSU rRNA) phylogenetics suggest that nematode phylogeny consists of five major clades (I to V) which include Dorylaimia (clade I), Enoplia (clade II) and Chromadorea (which includes Rhabditida; see Figure 1) (Gilleard, 2004; Parkinson *et al.* 2004). Rhabditida, a paraphyletic taxon, can further be divided into several other taxa including Spirurina (clade III), Tylenchina (clade IV) and Rhabditina (clade V) (Gilleard, 2004; Parkinson *et al.* 2004). Most clades are comprised of a combination of free-living nematodes as well as animal and plant parasites (Blaxter, 2002; Gilleard, 2004). Consequently, it is believed there have been multiple independent events of gain of parasitism during nematode evolution (Blaxter, 2002). Interestingly, clade III contains only animal parasites suggesting that parasitism is the ancestral state of this taxon (Blaxter, 2002).

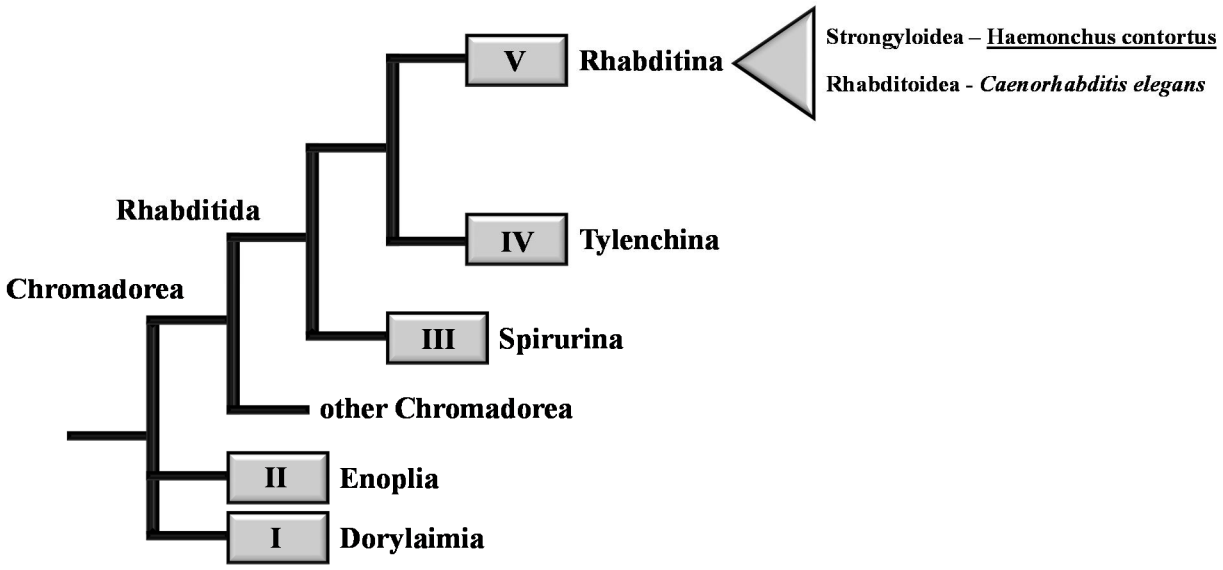

Figure 1. Phylogenetic tree showing evolutionary relationships within the phylum Nematoda. Species indicated are of great importance within this thesis. The evolutionary relationships are based on SSU rRNA sequences. The species underlined represents a parasitic nematode. The species shown in italics represent the related free-living nematode. Adapted from Gilleard (2004) and Parkinson *et al.* (2004).

One of the best known characteristics of the Nematoda is the vast number of parasitic species, many of which infect humans and domesticated animals (Blaxter, 2002). Thus, nematode infections represent a significant source of economical and health-related crises worldwide. Presently, it is estimated that approximately 2.9 billion people are inflicted with nematode infections resulting in a myriad of debilitating illnesses such as African river blindness and elephantiasis (Parkinson *et al.* 2004). The highest incidence rates are most commonly associated with tropical regions, especially that of Africa, Asia and the Americas (Parkinson *et al.* 2004). Consequently, it has been estimated that nematode-associated human morbidity rivals that of diabetes and lung cancer in worldwide disability adjusted life year (DALY) measurements (Parkinson *et al.* 2004). Fortunately mortality rates are low with respect to the incidence of infection; however, death rates may still exceed 100,000 annually. (Parkinson *et al.* 2004).

Another significant consequence to nematode infections is the substantial losses in livestock and companion animals. Major losses have been observed in the productivity within sheep wool and meat industries (Newton and Meeusen, 2003). In addition, nematode infections are responsible for approximately $80 billion in annual crop damage worldwide (Parkinson *et al.* 2004). Although nematode parasites infect an array of species, a vast majority of parasitic nematodes parasitize vertebrates, specifically mammals. The evolution of vertebrate parasitism has been quite successful, arising in at least four independent taxonomic groups: Trichocephalida (clade I), the three orders in clade III, the Strongyloididae (clade IV) and the Strongylida (clade V) (Dorris *et al.* 2002). Clade V is of high economical importance as this clade represents the strongylid nematodes; many of which are important veterinary pathogens (Gilleard, 2004). Most notable are the Trichostrongyloidea which include important parasitic nematode genera infecting domestic livestock such as *Haemonchus*, *Ostertagia*, and *Trichostrongylus*, (Gilleard, 2004).

1.1.1 Caenorhabditis elegans

The majority of our current understanding about the molecular and developmental biology of nematodes can be attributed to the nematode *Caenorhabditis elegans*. *C. elegans* is a free living soil nematode approximately 1 mm in length (Strange, 2006). This nematode is well adapted for survival in soil environments where it can outcompete its competitors by producing large numbers of offspring which in turn rapidly deplete local food sources (Strange, 2006). The sex of adult *C. elegans* is largely hermaphroditic with males comprising less than 0.1% of the wild-type populations (Strange, 2006).

As the first multi-cellular organism whose genome was completely assembled, *C. elegans* has been fundamental in medical research especially within the fields of cancer, ageing, neurobiology and parasitology (Parkinson *et al.* 2004). The scientific value of *C. elegans* is attributed to its simplistic life-cycle and ease of maintenance. Parasitic nematodes, unlike *C. elegans*, lack *in vitro* culture systems and require the propagation of life cycles *in vivo* (Gilleard, 2004). Alternatively, at 25°C, *C. elegans*' embryogenesis occurs in approximately 14 hours and post embryonic development (i.e. L1-L4 larval development) lasts a total of 35 hours (Strange, 2006). Furthermore, the typical life span of *C. elegans* is about 2-3 weeks. Thus, life-cycle experiments can be completed very rapidly. As a result, there is an increasing interest in the use of *C. elegans* as a standard tool for molecular helminthology (Gilleard, 2004).

For the wealth of information available regarding *C. elegans* there is comparatively little known about other members within this phylum. To date there are few studies directly comparing aspects of *C. elegans* biology with analogous processes in parasitic nematode species (Gilleard, 2004). One explanation for this lack of comparison is the extensive diversity of the phylum Nematoda (Gilleard, 2004). Thus, the value of *C. elegans* in helminthology will differ depending on its phylogenetic distance from a particular parasitic nematode species (Gilleard, 2004). For instance, *C. elegans* are located within clade V (Figure 1; Gilleard, 2004). Clade V also consists of strongylid nematodes, which as indicated previously, contain important parasitic nematode species infecting domestic livestock which include the *Haemonchus* family (Gilleard, 2004). As a result, *C. elegans*, a rhabditine nematode, is closely related to the vertebrate-parasite *Haemonchus contortus* (Parkinson *et al.* 2004). Thus it is reasonable to assume that *C.*

elegans biology will, in general, have more relevance to *H. contortus* than the more distantly related parasites within other clades.

1.1.2 Haemonchus contortus

One of the most economically important parasitic nematodes is *Haemonchus contortus* (Nikolaou and Gasser, 2006). *H. contortus* is a gastrointestinal parasitic nematode commonly infecting ruminants, such as sheep and cattle. The pathogenesis of a *Haemonchus* infection results from the bloodsucking activity of the parasite within the abomasum, or fourth stomach, of its host (Nikolaou and Gasser, 2006). *Haemonchus* infections may lead to serious health complications such as acute Haemonchosis or anaemia, which if left untreated, often leads to the animal's death (Nikolaou and Gasser, 2006).

The life cycle of *H. contortus* is complex consisting of two major phases: a free living and parasitic phase (Nikolaou and Gasser, 2006). Briefly, an adult hermaphrodite releases approximately 4,500 eggs within the abomasum of an infected host (Nikolaou and Gasser, 2006). These eggs develop to the 11-26 cell stage at which point oxygen becomes essential to proper development (Nikolaou and Gasser, 2006). Consequently, the eggs are released into the environment within the fecal matter and remain there until they develop into a developmentally arrested L3 infective larva (Nikolaou and Gasser, 2006). At this stage, the juvenile nematode waits on blades of grass to be consumed by a host. Upon being consumed, temperature, pH and chemical conditions within the host's gut stimulate the L3 larvae to attach to the mucosa of the abomasum initiating its parasitic life phase (Nikolaou and Gasser, 2006). The development of a buccal capsule

during the L4 larval stage is required to facilitate blood feeding (Nikolaou and Gasser, 2006). Finally, sexual differentiation of the juvenile parasite signals developmental completion (Nikolaou and Gasser, 2006).

At the moment, the most common treatment for *Haemonchus* infections is through the use of anthelmintics. There are several drugs used to treat *Haemonchus* infections and most target specific receptors of the parasite nervous system called ligand-gated ion channels (LGICs). Presently, there are three major classes of anthelmintics currently in use. The first class, the benzimidazoles, disrupt parasite tubulin polymerization. The levamisole/morantel family disrupt sodium transport through cholinergic receptor channels. Finally the avermectins, consisting of macrocyclic lactones (i.e. Ivermectin, IVM), activate glutamate-gated chloride channels that are present on nematode neuromuscular systems (Mes, 2004). As a result, parasitic nematodes are effectively paralyzed.

Unfortunately the development of genetic resistance (i.e. anthelmintic resistance) to several of these drugs in *H. contortus* is an unwanted consequence of the evolutionary process. Genetic resistance within a population is perpetuated to the next generation via the survival of a parental line under selective pressures such as anthelmintic treatment (Njue and Prichard, 2004). Ultimately, the frequency of resistant individuals within the population will increase resulting in overall treatment failure (Njue and Prichard, 2004; Blackhall *et al.* 2008).

1.1.3 C. elegans as a model for H. contortus

As the rise of resistance to several anthelmintics in *H. contortus* continues to reduce treatment efficacy, the need for novel treatment development has increased. As a result, there is growing interest in the use of the free-living nematode *C. elegans* as a standard tool for molecular helminthology (Gilleard, 2004). However, there currently is an ongoing debate regarding the relevance of *C. elegans* biology in parasitology, especially with respect to *H. contortus* (Gilleard, 2004). Therefore, in order to use this understanding to develop novel drug treatments for nematode-induced diseases, the relationship between *C. elegans* and *H. contortus* must be understood. Previous studies have demonstrated that *C. elegans* can be used to study *H. contortus* biology at the molecular level. For instance, the *H. contortus* isotype 1 β-tubulin gene (*tub-1*), involved in benzimidazole resistance, was the first parasite gene to be functionally expressed under the control of its own *cis* regulatory elements in *C. elegans* (Kwa *et al.* 1995). This approach provided a functional assay to test putative benzimidazole resistance-conferring alleles from the parasitic nematode *H. contortus* (Kwa *et al.* 1995; Gilleard, 2004). Moreover, transforming *C. elegans ben-1*, benzimidazole resistant, mutants with susceptible alleles of the *H. contortus tub-1* genes increased sensitivity of the strain to benzimidazoles (Kwa *et al.* 1995). This work exemplifies how an interspecies mutant rescue experiment allows for a parasite gene to be functionally examined in some detail (Kwa *et al.* 1995; Gilleard, 2004).

Studies involving GABA receptor gene co-expression between *C. elegans* and *H. contortus* have also been conducted. A LGIC receptor subunit known as Hco-LGC-37 has been identified in *H. contortus* which can only form GABA sensitive channels in

Xenopus laevis oocytes in the presence of a $GABA_A$ β-like receptor subunit (Feng *et al.* 2002). As a result, when the Hco-LGC-37 subunit was co-expressed with a *C. elegans* β-like receptor subunit, known as GAB-1, a fully functional heteromeric GABA-sensitive channel was produced (Feng *et al.* 2002). Thus, this investigation demonstrated the potential for interspecies gene co-expression studies for exploring the function of parasite LGIC receptor subunits.

1.2 Ligand-gated Ion Channels

Fast synaptic neurotransmission, both excitatory and inhibitory, for invertebrates and vertebrates is mediated in part by the nicotinic class of LGIC receptors (Johnston, 2005). LGICs, also called cysteine-loop (Cys-loop) receptors (Mes, 2004), can be subdivided into cation- and anion-selective channels (Johnston, 2005). Excitatory receptors are generally activated by molecules such as acetylcholine or serotonin whereas inhibitory receptors are generally activated by γ-aminobutyric acid (GABA), glutamate (only in invertebrates) or glycine (Yates *et al.* 2003; Johnston, 2005). Both cationic and anionic receptors can form homomeric receptors in which five copies of a single type of subunit assemble together (Johnston, 2005). However, LGICs more commonly assemble from several different types of subunits forming hetero-pentamers (Johnston, 2005). These pentamers are composed of five subunits which are arranged in the post-synaptic membrane to form a central ion channel (Johnston, 2005). Each subunit consists of an N-terminal extracellular domain wherein the ligand binding sites reside, four transmembrane domains (TM1-TM4) - the second of which form the channel-lining, and an extracellular C-terminus (Johnston, 2005; see Figure 2). Due to numerous subunit

types, there can be a large variety of possible heteromeric channels which in turn offers a myriad of functional diversity able to meet a wide range of synaptic needs (Johnston, 2005).

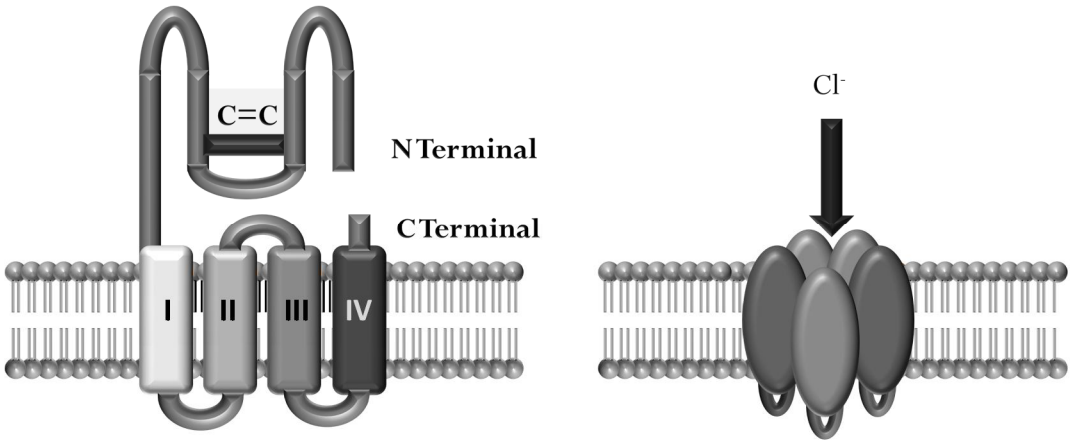

Figure 2. Schematic structure of LGIC receptors. Left: Monomeric subunit located within a cellular membrane. The cellular membrane is represented by the lipid bi-layer. The transmembrane regions are located within the cellular membrane depicted by shaded rectangles. TM1 is located on the far left (I) and TM4 is located on the far right (IV). TM2 and 3 are positioned accordingly. The characteristic disulfide bond of the Cys-loop family of receptors is located in the N-terminal extracellular domain depicted as a black line. **Right:** A representative illustration of five subunits symmetrically arranged around the central pore. The ions which pass through the central pore are dependent upon the receptor class. For clarity, chloride ions were chosen to indicate passage through the channel pore. Adapted from Lester *et al*. (2004).

Due to the high degree of functional diversity within the LGIC superfamily, a variety of LGICs have been described in both vertebrates and invertebrates. The function of each receptor has evolved to meet a specific synaptic role. For instance, nicotinic acetylcholine receptors (nAChRs) and serotonin-gated cation channels (5-HT_3) are both expressed in nerve cells while the former is additionally expressed in muscle cells (Connolly and Wafford, 2004). Consequently, both receptors play an essential role in fast synaptic cationic neurotransmission (Connolly and Wafford, 2004). Conversely, the glycine and GABA receptor are part of the inhibitory nervous system and as such are expressed within the spinal cord and central nervous system, respectively (Connolly and

Wafford, 2004). Additionally, invertebrate systems have been shown to express ligand-gated chloride channels (LGCC) which are activated by non-traditional neurotransmitters such as histamine (Gisselmann *et al.* 2001), glutamate (Cully *et al.* 1994), dopamine (Rao *et al.* 2009) and tyramine (Pirri *et al.* 2009).

The activation of LGICs has been linked to six discontinuous extracellular loops within the extracellular N-terminal (Kash *et al.* 2004, Lummis, 2009). This N-terminal loop model appears to be well conserved across a wide variety of LGICs and contains the ligand (neurotransmitter) binding pocket (Kash *et al.* 2004). Channel opening is initiated by neurotransmitter binding which causes constriction of the binding pocket (Kash *et al.* 2004). This constriction causes a 'conformational wave' of several loops within the extracellular structure resulting in interactions between the TM2–3 linker and pre-TM1 segments (see Figure 2; Kash *et al.* 2004). Subsequently, both a rotation and tilting of the TM helices allows the channel pore to open (Kash *et al.* 2004).

1.3 GABA-gated Chloride Channels

The most abundant inhibitory neurotransmitter in vertebrate nervous systems is GABA (Schuske *et al.* 2004), which is estimated to be present in approx 20-50% of cerebral cortex synapses (Hevers and Lüddens, 1998). Thus, it is of no surprise that GABA has been implicated in numerous psychiatric disorders such as anxiety, insomnia and epilepsy (Hevers and Lüddens, 1998). GABA invokes neuronal inhibition by acting on three classes of membrane-bound receptors encoded within the vertebrate genome (Johnston, 2005). These receptors can be divided into two major types: ionotropic receptors ($GABA_A$ and $GABA_C$ receptors) and metabotropic receptors that are G-protein

coupled receptors ($GABA_B$ receptors; Hevers and Lüddens, 1998; Johnston, 2005); the latter acts via second messengers (Johnston, 2005). However, it is the fast inhibitory synaptic neurotransmission, mediated by ionotropic GABA receptors, which play the most extensive roles in regulating mechanisms within the nervous system of both vertebrates and invertebrates (Lee *et al.* 2003).

The ionotropic GABA receptors are members of the nicotinic-like LGIC superfamily, which form pentameric complexes arranged around a central ion conducting pore (Johnston, 2005). Similar to all members of the LGIC, these GABA receptors are composed of a large extracellular N-terminal domain and four transmembrane domains (Johnston, 2005). The cytoplasmic loop, between the third and fourth transmembrane domains of the receptor is thought to be the target for protein kinases, required for sub-cellular targeting and membrane clustering (Johnston, 2005). $GABA_A$ and $GABA_C$ receptors assemble into chloride-selective transmembrane channels ubiquitously distributed within the central nervous system (CNS) of vertebrates where their main physiological role is the mediation of inhibitory neurotransmission (Hevers and Lüddens, 1998; Johnston, 2005).

1.3.1 The Vertebrate $GABA_A$ Receptor

Of all the receptors which constitute the LGIC superfamily, the $GABA_A$ receptor represents one of the most thoroughly characterized receptors in the vertebrate nervous system. $GABA_A$ receptors embody a sophisticated and complex receptor family comprised of 16 different subunits: α_{1-6}, β_{1-3}, γ_{1-3}, δ, ε, π and θ (Johnston, 2005). As a result $GABA_A$ receptors have the ability to form either homomeric or, more commonly,

heteromeric channels. Many of the subunits also have possible splice variants which increase the overall complexity and receptor variability (Johnston, 1996). Consequently, $GABA_A$ receptors have the potential to form thousands of functional pentameric receptors with diverse subunit arrangements (e.g. α_1, β_2 and γ_2 subunits). Over 2000 different pentameric $GABA_A$ receptors could exist even if combinations were restricted to those containing at least two α and two β subunits (Johnston, 2005). However, different neuron classes appear to express specific combinations of subunit genes with roughly a dozen major $GABA_A$ receptor subtypes identified experimentally (McKernan and Whiting, 1996). Thus, it appears that the number of $GABA_A$ receptor subtypes is constrained by subunit expression patterns indicating that the formation of these receptors is a highly regulated process (Bamber *et al.* 1999).

$GABA_A$ receptors are one of the most complicated receptors found in the LGIC superfamily not only in terms of the large number of receptor subtypes but also the large variety of ligands which interact with specific sites on the receptor (Johnston, 1996). It is estimated that approximately 11 distinct ligand binding sites are located on the $GABA_A$ receptor which associate with more than 100 different known agents such as GABA, picrotoxin (PTX), muscimol, bicuculline and propofol (Johnston, 1996). Although the number of specific sites may vary, depending upon the subunit arrangement, all receptors must contain at least one β-subunit to form a properly functioning receptor (Amin and Weiss, 1993; Johnston, 1996). This is a result of two separate and homologous domains on the β-subunit which are essential for activation by GABA (Amin and Weiss, 1993). These homologous domains, known as binding domains I and II (BDI and BDII, respectively), are both four amino acids in length and each contribute a tyrosine and

threonine essential in the binding of a GABA molecule (Amin and Weiss, 1993). These amino acids are highly conserved across a wide spectrum of species due to their essential roles in the activation of $GABA_A$ receptors (see Table 1). Both the tyrosine and threonine are said to form hydrogen-bonds between the main chain amino and the carboxyl groups (Amin and Weiss, 1993). Additionally, a conserved glycine is said to assist in the formation of hairpin turns aligning the tyrosine and threonine in close proximity to the agonist (Amin and Weiss, 1993).

Table 1. Comparative analysis of GABA receptor binding loop sequences from several species.

Species	Common Name	Vertebrate	Receptor/Subunit	Loop B[1] BDI Sequence	Loop C[1] BDII Sequence	Loop D Sequence	Reference
Homo sapiens	Human	Yes	$GABA_A$/β-subunit	ES**YGYT**T	VVFS**TGSY**P	LTMYFQQA	Schofield *et al.* 1987
Rattus norvegicus	Rat	Yes	$GABA_A$/β-subunit	ES**YGYT**T	VVFS**TGSY**P	LTMYFQQY	Lolait *et al.* 1989
Bos Taurus	Bovine	Yes	$GABA_A$/β-subunit	ES**YGYT**T	VVFS**TGSY**P	LTMYFQQA	Ymer *et al.* 1989
Gallus gallus	Chicken	Yes	$GABA_A$/β-subunit	ES**YGYT**T	VVFA**TGAY**P	LTMYFQQY	Bateson *et al.* 1990
Caenorhabditis elegans	Roundworm	No	UNC-49/B-subunit	ES**YGYE**T	AETS**SGKY**V	LDFYMRQT	Bamber *et al.* 1999
Haemonchus contortus	Barber Pole Worm	No	UNC-49/B-subunit	ES**YGYT**M	ATTS**SGSY**R	LDFYMRQT	Siddiqui e*t al.* 2010
Drosophila melanogaster	House Fly	No	RDL/isoform B	ES**FGYT**M	INLT**TGNY**S	LDFYFRQF	ffrench-Constant *et al.* 1991
Lymnea stagnalis	Pond Snail	No	$GABA_A$/β-like subunit	ES**YGYT**M	EELS**TGDY**Q	ITMYLNQY	Harvey *et al.* 1991

[1] The bolded amino acids, within each respective loop sequence, denote the putative binding domains

The complexity of GABA binding in $GABA_A$ receptors is attributed to the fact that the GABA binding site is located at subunit interfaces (Lummis, 2009). Based on structural modelling of the related acetylcholine binding protein (AChBP) it has been demonstrated that, like other Cys-loop receptors, the entire binding pocket of the $GABA_A$ receptor is constructed from six regions, known as Loops A-F (Lummis, 2009; see Figure 3A). In fact, the formation of the ligand-binding site appears to be composed of residues contributed from Loops A-C of the principle subunit and residues from Loops D-F of the adjacent subunit (Lummis, 2009). For instance, the most common $GABA_A$ receptor observed in the vertebrate nervous system is composed of α_1, β_2 and γ_2 subunits (McKernan and Whiting, 1996). From this composition it has been shown through mutagenesis that residues critical for binding can be found in Loop B (β_2Tyr^{157} and β_2Thr^{160}; BDI residues) and C (β_2Thr^{202} and β_2Tyr^{205}; BDII residues) of the principle subunit and Loop D (α_1Phe^{64}) of the adjacent subunit (Sigel *et al.* 1992; Amin and Weiss, 1993; Lummis, 2009; see Figure 3B). Additionally, other loops have been shown to be involved in GABA sensitivity within the β_2-α_1 interface such as Loop A (β_2Tyr^{97}; Boileau *et al.* 2002), E (α_1Arg^{120}; Westh-Hansen *et al.* 1999), and F (α_1Asp^{181}; Newell and Czajkowski, 2003).

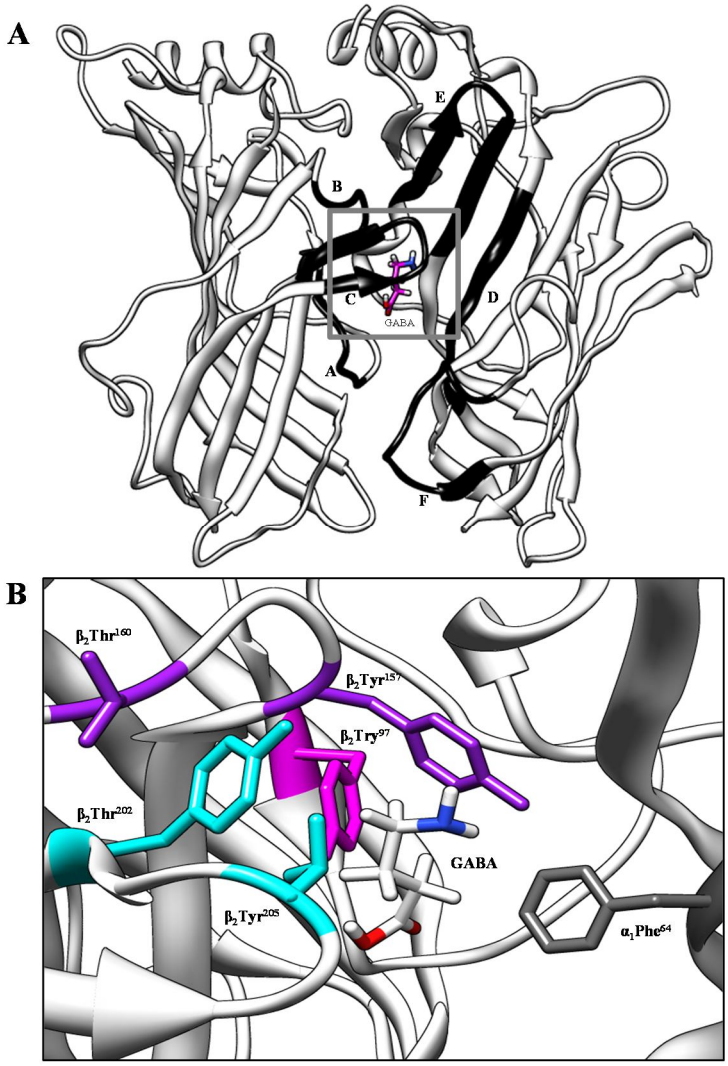

Figure 3. Model of the $GABA_A$ receptor β_2-α_1 subunit interface. A) Docking of GABA into the β_2-α_1 subunit interface. The β_2 subunit is located on the left. The α_1 subunit is located on the right. The six discontinuous loops involved in the binding of GABA are highlighted in black and identified with their corresponding letter designation. The grey box represents the areas enlarged in Figure 3B. B) Amino acids (represented in their stick form) shown to be essential for GABA binding in the $GABA_A$ receptor. Amino acid loop designations are identified as follows: Loop A (magenta), Loop B (purple), Loop C (cyan). Loop D (dark gray). The blue colour on the GABA molecule represents the nitrogen atom. The red colours on the GABA molecule represent oxygen atoms.

1.3.2 The Invertebrate GABA Receptors

Similar to their vertebrate counterparts, invertebrate ionotropic GABA receptors can be found dispersed throughout the nervous system of many insects and worms (Hosie *et al.* 1997). Invertebrate ionotropic GABA receptors form anion-selective ion channels

which perform rapid synaptic inhibitory neurotransmission (Hosie *et al.* 1997). Although both vertebrate and invertebrate ionotropic GABA receptors share similar functional and structural characteristics, their pharmacological profiles are quite different (Hosie *et al.* 1997). For instance, vertebrate $GABA_A$ receptors are antagonized by both bicuculline and PTX (Hosie *et al.* 1997). Although some invertebrate ionotropic GABA receptors are also antagonized by PTX, they are typically insensitive to bicuculline (Hosie *et al.* 1997). In fact, invertebrate ionotropic GABA receptors differ from both vertebrate $GABA_A$ and $GABA_C$ receptors in their sensitivity to many GABA analogues and allosteric modulators (Hosie *et al.* 1997).

In contrast to what is known regarding vertebrate GABA receptors, there have been only a limited number of GABA receptor subunits cloned and characterized from invertebrate organisms. Thus far there have been three Cys-loop receptor subunit classes identified in *Drosophila melanogaster* (common fruit fly). The three classes are encoded by three genes: the *glycine-like receptor of Drosophila* (*Grd*), the *ligand-gated chloride channel homologue 3* (*Lcch3*), and the *resistance to dieldrin like* (*Rdl*) (Hosie *et al.* 1997). However, the most extensively characterized non-vertebrate GABA receptor is the major product of the *Rdl* gene, the RDL receptor (Hosie *et al.* 1997).

The *Rdl* gene has the ability to produce four possible gene products all possessing features characteristic of ionotropic GABA receptors (Hosie *et al.* 1997). In fact, the subunits encoded within the *Rdl* gene display approximately 30-38% sequence identity to that of vertebrate $GABA_A$ β-subunits and $GABA_C$ ρ-subunits – which is typical sequence identity for vertebrate verses invertebrate GABA receptors (Hosie *et al.* 1997). Moreover, the RDL receptor has the ability to form homomeric channels, a feature characteristic of

$GABA_A$ β-subunits and $GABA_C$ ρ-subunits (Hosie *et al.* 1997). Immunocytochemical studies indicated that the *Rdl* gene products are in fact distributed throughout the *Drosophila* CNS and concentrated in regions of neuropil (Hosie *et al.* 1997). Furthermore, it appears that the distribution of RDL antibody staining correlates closely with that of immunoreactivity for GABA, as well as for the enzyme glutamic acid decarboxylase and the synaptic vesicle protein synaptotagmin (Hosie *et al.* 1997). Thus, the evidence convincingly implements the *Rdl* gene products, specifically the RDL protein, as synaptic neuronal GABA receptors (Hosie *et al.* 1997). Partial and full-length complementary deoxyribonucleic acids (cDNAs) encoding homologues of the *Drosophila* RDL subunits have further been identified in species within three orders of insects including: the yellow fever mosquito *Aedes aegypti* (Diptera), the German cockroach *Blattella germanica* (Dictyoptera), and the beetle *Tribolium castaneum* (Coleoptera) (Hosie *et al.* 1997).

With respect to nematodes there have been several GABA receptors characterized. Previous studies on *H. contortus* have identified a GABA receptor subunit gene called *Hco-lgc-37* (Laughton *et al.* 1994) which is expressed in ring motor- and inter-neurons (Skinner *et al.* 1998). Functional analysis indicates that while Hco-LGC-37 does not form a functional homomeric channel, it can co-assemble with the *C. elegans* subunit Cel-GAB-1 to form a functional GABA-sensitive channel (Feng *et al.* 2002). Recently, a RDL homologue was isolated from *H. contortus* (Hco-LGC-38; Siddiqui *et al.*, unpublished). However, to date, it is unknown in which tissues these receptor subunits are expressed (Siddiqui *et al.*, unpublished). Other nematode GABA receptors

include the UNC-49 GABA receptors which are discussed below.

1.4 The Uncoordinated Genes

The importance of the GABAergic nervous system in nematodes was first determined through investigations in which laser ablation was conducted on 26 of the 302 neurons present in *C. elegans* which express the neurotransmitter GABA (McIntire *et al.* 1993a). When the dorsal and ventral D-type motor neurons (DD or VD, respectively) were ablated, *C. elegans* exhibited abnormal locomotion (McIntire *et al.* 1993a). Typically when a *C. elegans* travels, muscle contractions on one side of the body cause the body to bend whilst simultaneous muscle relaxation, via GABA innervations, occurs on the opposite side (Schuske *et al.* 2004). As a result, movement is driven through a sinusoidal body wave. However, if laser ablation is used to kill the VD and DD neurons required for relaxation of body wall muscles, the operated worm has only excitatory input into its muscles (Schuske *et al.* 2004). Hence locomotion becomes abnormal. The resultant phenotype, known as a 'shrinker' phenotype, occurs as the worm pulls its head in and its body shortens owing to hypercontraction of the body wall muscles on both sides of the body (Schuske *et al.* 2004).

In nematode locomotion, GABA release from the VD neurons is essential for muscle relaxation to reset posture when changing directions (Schuske *et al.* 2004). If GABA is not properly utilized, locomotion becomes 'uncoordinated' and the shrinker phenotype develops. It is from this understanding that five uncoordinated (*unc*) genes, required for GABA function, were identified in *C. elegans* mutants which resembled the shrinker phenotype after laser ablation (Schuske *et al.* 2004). Three *C. elegans* mutants,

unc-25, *unc-46* and *unc-47*, appear to shrink and lack enteric muscle contractions (Schuske *et al.* 2004). This suggests the mutated genes encode proteins that are required for both inhibitory and excitatory GABA functions (Schuske *et al.* 2004). Additionally, two other mutants, *unc-30* and *unc-49*, solely display the 'shrinker' phenotype signifying that the associated proteins are required only for inhibitory GABA function (Schuske *et al.* 2004).

McIntire *et al.* (1993b) used the GABA receptor agonist muscimol to determine whether the *unc* gene products were pre- or post-synaptic. If the *unc* gene encoded a protein required in the presynaptic neuron, muscles in the *C. elegans* mutants would respond normally to muscimol (McIntire *et al.* 1993b; Schuske *et al.* 2004). Accordingly, muscimol will activate postsynaptic GABA receptors constitutively (Schuske *et al.* 2004). When McIntire *et al.* (1993b) bathed wild-type worms in muscimol, contractions ceased in the body muscles causing the animal to become flaccid. This effect was seen with the muscimol sensitive mutants: *unc-25, unc-30, unc-46* and *unc-47* (McIntire *et al.* 1993b; Schuske *et al.* 2004). It was later discovered that these genes encoded the biosynthetic enzyme for GABA - glutamic acid decarboxylase, a homeodomain transcriptional factor required for GABA neuronal specification in the D-type neurons, a gene which regulates the transport of GABA into vesicles and the vesicular GABA transporter (VGAT), respectively (McIntire *et al.* 1993b; Jin *et al.* 1994; Jin *et al.* 1999; Schuske *et al.* 2004; see Figure 4). However, the *unc-49* mutant was resistant to the effects of muscimol on the body suggesting this gene encodes postsynaptic GABA receptors (McIntire *et al.* 1993b). Since the *unc-49* mutants were defective only for

locomotion (an inhibitory GABA function), this gene was predicted to encode an inhibitory GABA receptor (Schuske *et al.* 2004).

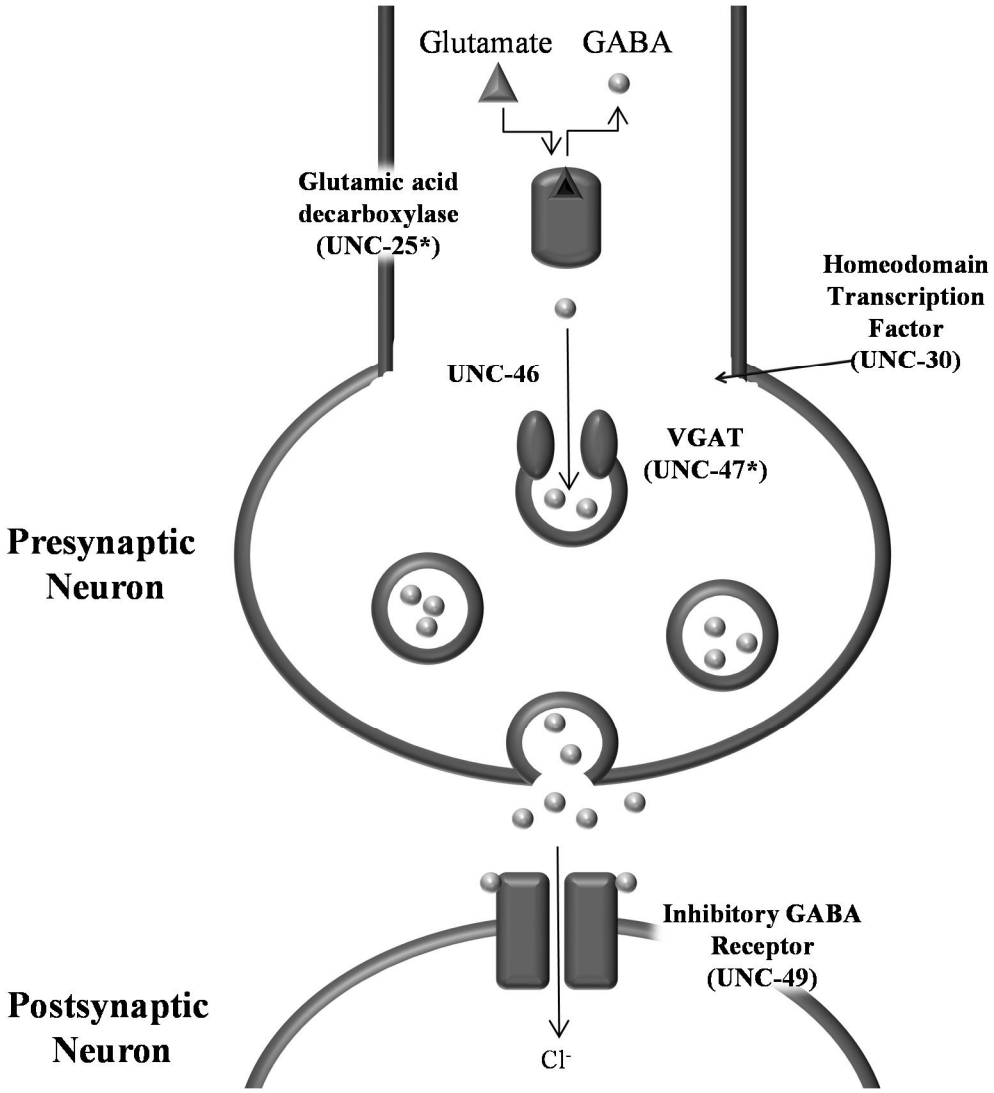

Figure 4. Uncoordinated proteins required for GABA synthesis and transport in *Caenorhabditis elegans*. GABA is synthesized from glutamate by the *unc-25* gene product - glutamic acid decarboxylase. GABA is then transported into synaptic vesicles via the vesicular GABA transporter (VGAT), a protein encoded by the *unc-47* gene. It is proposed UNC-46 modulates vesicular GABA loading. UNC-30, a homeodomain transcription factor, is necessary for UNC-25 and UNC-47 expression as denoted by the asterisk. Finally, GABA is released from the neuron activating the inhibitory GABA receptor UNC-49 increasing Cl_2 uptake and thus relaxing body muscles. Adapted from Schuske *et al.* (2004).

1.4.1 C. elegans UNC-49 GABA Receptor

C. elegans mediate body muscle inhibition during locomotion by means of the GABA receptor encoded by the *unc-49* gene (Schuske *et al.* 2004). The *unc-49* gene locus possesses a gene structure which encodes three distinct GABA receptor subunits. Through alternative splicing, a common N-terminal ligand binding domain is spliced to one of three potential C-terminal domains (Bamber *et al.* 1999). As a result, three different *C. elegans* GABA receptor subunits (Cel-UNC-49A, Cel-UNC-49B and Cel-UNC-49C) are produced (Bamber *et al.* 1999). This unusual gene structure is also conserved in the related nematode *Caenorhabditis briggsae* (Schuske *et al.* 2004).

Of the three aforementioned Cel-UNC-49 subunits, Cel-UNC-49A is barely detectable *in vivo* (Bamber *et al.* 1999). Additionally, it has been shown that Cel-UNC-49A does not co-assemble with Cel-UNC-49B or Cel-UNC-49C to form a functional heteromeric receptor *in vitro* (Bamber *et al.* 1999). Alternatively, strong expression of the Cel-UNC-49B and Cel-UNC-49C subunits has been identified at neuromuscular junctions from the D-type GABA motor neurons (Bamber *et al.* 1999; Schuske *et al.* 2004). Electrophysiological studies have demonstrated that Cel-UNC-49B subunits can form functional homomeric receptors, whereas Cel-UNC-49C cannot (Bamber *et al.* 1999). However, the two subunits can associate to form functional heteromeric channels when co-expressed in *Xenopus laevis* oocytes indicating that a UNC-49B/C heteromer may be the native receptor *in vivo* (Bamber *et al.* 1999). This was later confirmed through *in vivo* studies which detected the heteromeric channel at the neuromuscular junction (Bamber *et al.* 2005).

To better understand the pharmacological properties of UNC-49 GABA receptors, it is essential to understand their relationship to other LGICs. Phylogenetic analysis indicates that UNC-49 subunits are closely related to the RDL receptors of *Drosophila melanogaster* (Bamber *et al.* 2003). Although vertebrate $GABA_A$ receptors and UNC-49 receptors are related, the UNC-49 subunits are not orthologues to any class of $GABA_A$ receptor subunits (Bamber *et al.* 2003). However, like RDL receptors, UNC-49 subunits do share some sequence similarity with specific $GABA_A$ receptor subunits. UNC-49B and UNC-49C share roughly 35-45% sequence similarity with that of mammalian α, β, γ and ρ subunits: UNC-49B shares 42.5% similarity with the $GABA_A$ β subunit (Bamber *et al.* 2003).

When comparing the pharmacology of the UNC-49 GABA receptors with that of mammalian GABA receptors there are key differences observed that appear to be linked to structural differences between the channels. For instance, Bamber *et al.* (2003) demonstrated that Cel-UNC-49B homomers are sensitive to PTX, whereas Cel-UNC-49B/C heteromers were resistant. This change in PTX sensitivity has been attributed to a single residue within the M2 domain (Gurley *et al.* 1995; Bamber *et al.* 2003; Schuske *et al.* 2004). Gurley *et al.* (1995) showed that the conserved threonine at the 6' position in the M2 domain is essential in determining PTX sensitivity in the rat ρ1 $GABA_C$ receptor subunit. A mutation replacing the threonine with a methionine in the rat ρ1 $GABA_C$ receptor subunit resulted in PTX resistance (Gurley *et al.* 1995). In fact, the Cel-UNC-49C subunit contains a methionine in this position which confers PTX resistance to the Cel-UNC-49B/C heteromer (Bamber *et al.* 2003). Conversely, the Cel-UNC-49B subunit possesses the aforementioned conserved threonine at the 6' position resulting in a PTX

sensitive channel when it is assembled as a homomeric channel (Bamber *et al.* 2003).

1.4.2 H. contortus UNC-49 GABA Receptor

Recently, two orthologous Cel-UNC-49 subunit genes were isolated in *H. contortus* known as Hco-UNC-49B and C. Structure-function analysis has shown that the Hco-UNC-49 subunits share similar characteristics with those observed in *C. elegans*. For instance, the Hco-UNC-49 subunits have been shown to possess similar N-terminal amino acid sequences whereas their C-terminal sequences exhibit some variability. Thus, it is believed that the Hco-UNC-49 gene transcripts are under the same alternative splicing mechanisms as their Cel-UNC-49 counterparts. Furthermore, like their *C. elegans* orthologues, the Hco-UNC-49C subunit is unable to form a functional homomeric channel, yet possesses the ability to form a functional PTX resistant heteromeric channel when co-expressed with Hco-UNC-49B (Siddiqui *et al.* 2010).

The most interesting characteristic of the Hco-UNC-49 receptor is its relative sensitivity to GABA compared to the Cel-UNC-49 receptor. Specifically, the Hco-UNC-49B/C heteromeric channel exhibits an increased GABA sensitivity compared to that of the Hco-UNC-49B homomeric channel (EC_{50} of 39.9 ± 5.7 μM to 64.0 ± 4.4 μM, respectively; Siddiqui *et al.* 2010) – a trend which was opposite in *C. elegans*. Additionally, the Hco-UNC-49B/C heteromer is approximately 2.5 times more sensitive to GABA than the Cel-UNC-49B/C heteromer; a feature which may be indicative of a requirement for a more sensitive receptor by the parasite *in vivo*. In addition, through experiments which combined Cel-UNC-49 and Hco-UNC-49 receptor subunits, it was demonstrated that Hco-UNC-49B was essential for this increased sensitivity. However,

the understanding as to why there is an increase in GABA sensitivity with Hco-UNC-49B-associated heteromeric channels remains unclear (Siddiqui *et al.* 2010). One potential cause may be the amino acid differences within the BDs of the *C. elegans* and *H. contortus* receptors.

Overall, there are current gaps in our understanding of the relative importance of the putative binding loops and binding domains of the UNC-49 receptor for the activation of the channel by GABA. In addition, it is not known whether these BDs can explain the observed differences in GABA sensitivity between *H. contortus* and *C. elegans* UNC-49 receptors. This represents a substantial gap in scientific knowledge which warrants further research. Any information obtained in this investigation will present a novel understanding of the elements required in the activation of nematode GABA receptors.

1.5 Objectives

The aim of this study was to investigate which amino acids are essential for GABA sensitivity in the *H. contortus* UNC-49 GABA receptor. The focus here was on Loops B, C and D which are three of the six loops that have been identified in other organisms as important for GABA sensitivity. A variety of amino acids, identified as essential for GABA binding to mammalian $GABA_A$ receptors, were mutated via site-directed mutagenesis. In addition, a parallel study examined whether observed differences in GABA sensitivity between the *H. contortus* and *C. elegans* UNC-49 receptors is the result of amino acid differences in the putative BDs found in Loops B and C. Specifically, mutations were introduced into the BDs of the *H. contortus unc-49* gene in order to change the amino acid to what is present in the *C. elegans'* UNC-49 receptor.

In all cases, the effect of each mutation was examined by two-electrode voltage clamp electrophysiology. Those mutations that caused a substantial affect on GABA sensitivity were also analyzed via homology modelling.

The goal of this research is to better understand how key binding residues in nematode GABA receptors determine function. In doing so, this investigation will also provide valuable information of the evolution of these primitive channels and may reveal clues on the relationship between the *H. contortus* UNC-49 GABA binding pocket and that of the *C. elegans* UNC-49 and vertebrate $GABA_A$ receptors.

Chapter 2 – Molecular Characterization of the Binding Site of Nematode $GABA_A$ Receptors

2.1 Introduction

Fast synaptic neurotransmission in both vertebrate and invertebrate systems is mediated, in part, by a large superfamily of ligand-gated ion channels known as Cys-loop receptors. In mammals, the Cys-loop superfamily can be broadly categorized as excitatory receptors (nicotinic acetylcholine, 5-HT_3) and inhibitory receptors (glycine, γ-aminobutyric acid or GABA; Miller and Smart, 2010). In nematodes, such as the model organism *Caenorhabditis elegans*, inhibitory neurotransmission is predominately mediated by ionotropic GABA receptors (referred to as UNC-49 receptors) which are concentrated at neuromuscular junctions wherein their physiological role is the GABA-mediated control of locomotion (Bamber *et al.* 1999). These nematode $GABA_A$ receptors differ considerably from mammalian $GABA_A$ receptors in sequence homology, pharmacology and overall function. The *unc-49* gene encodes for three subunits (UNC-49A, UNC-49B and UNC-49C) which are involved in *C. elegans* locomotion (Bamber *et al.* 1999). However, only UNC-49B and UNC-49C are expressed at physiologically relevant levels and co-assemble to form the native receptor *in vivo* (Bamber *et al.* 1999; Bamber *et al.* 2005).

Recently, two orthologues of the *Cel-unc-49* genes (*Hco-unc-49B* and *Hco-unc-49C*) were identified in the related parasitic nematode *Haemonchus contortus* (Siddiqui *et al.* 2010). Although there is a high degree of amino acid sequence homology between the receptors in the two species, there are pharmacological differences. Notably, the *H. contortus* heteromeric channel has approximately a 2.5-fold higher sensitivity to GABA compared to the *C. elegans* channel (Siddiqui *et al.* 2010). In addition, UNC-49C appears to be a positive modulator of GABA sensitivity in the *H. contortus* heteromeric

channel, but is a negative modulator of GABA sensitivity in the *C. elegans* heteromeric channel (Bamber *et al.* 1999; Siddiqui *et al.* 2010). These differences may be attributed to differences within the putative binding pocket of each receptor. However, the exact identity of the essential elements involved in GABA sensitivity in nematode $GABA_A$ receptors is largely unknown.

Knowledge regarding the molecular elements required for mammalian $GABA_A$ receptor activation has stemmed from mutational analysis, photoaffinity labelling, radioligand-binding assays and *in silico* homology modelling studies (Sigel *et al.* 1992; Amin and Weiss, 1993; Smith and Olsen, 1994; Cromer *et al.* 2002; Boileau *et al.* 2002). From these studies it is generally accepted that the GABA binding site is comprised of the interactions between six discontinuous loops (Loops A-F) found within the extracellular domains of interacting subunits; Loops A-C of the principle subunit and Loops D-F of the adjacent subunit (Lummis, 2009). These loops can be readily observed in homology models that have been generated using the low resolution extracellular structure of the related acetylcholine binding protein (AChBP; Boileau *et al.* 2002; Sixma and Smit, 2003; Padgett *et al.* 2007; Lummis, 2009). The validity of these homology models have been demonstrated in parallel mutagenesis and radioligand-binding assay studies which have identified key residues within these loops that are essential for ligand binding (Sigel *et al.* 1992; Amin and Weiss, 1993; Smith and Olsen, 1994; Cromer *et al.* 2002; Boileau *et al.* 2002).

Homology modelling of invertebrate Cys-loop receptors has been limited even though these receptors have been shown to be important targets for both pesticides and anthelmintics (Casida, 1993; Casida, 2009; McGonigle and Lummis, 2010). Very

recently, a 3-dimensional homology model of the most thoroughly studied insect GABA receptor, the *Drosophila melanogaster* RDL receptor, was constructed and used to study the binding of several GABA analogues (McGonigle and Lummis, 2010). This study revealed key binding structures within the RDL receptor, several of which are analogous to vertebrate $GABA_A$ receptors (McGonigle and Lummis, 2010). Invertebrate receptor studies such as these are key to providing insight into the similarities and differences between the invertebrate and mammalian GABA binding pocket. This will be important for an enhanced understanding of the evolution of GABA neurotransmission and possibly the discovery of novel pesticides and anthelmintics.

Analysis of the extracellular domain of the nematode UNC-49 $GABA_A$ receptor has revealed the presence of sequences that are homologous to the six binding loops known to be crucial for vertebrate $GABA_A$ receptor activation. Thus, the aim of this study is evaluate the importance of these loops for UNC-49 channel activation. Through site-directed mutagenesis and homology modelling, this study has uncovered several amino acid residues that are important for GABA sensitivity and appear to have analogous functions to what has been reported for mammalian receptors. Intriguingly however, several mutations have unveiled potential differences in the binding pocket between nematode and mammalian $GABA_A$ receptors. Finally, there is at least one amino acid that may partially account for the observed differences in GABA sensitivity between *H. contortus* and *C. elegans* UNC-49 channels.

Chapter 3 –
Materials and Methods

3.1 Mutation introduction and in vitro transcription of Hco-UNC-49

The coding sequences of Hco-UNC-49B and Hco-UNC-49C were sub-cloned into a pT7TS transcription vector. This transcription vector incorporates *Xenopus laevis β*-globin untranslated DNA to the 5' and 3' end of the *unc-49* gene (Dent *et al.* 1997). Mutagenic primers, that introduce single nucleotide changes in the *Hco-unc-49B* and *Hco-unc-49C* coding sequence, were designed using Stratagene's web-based QuikChange® Primer Design Program (http://www.stratagene.com/sdmdesigner/default.aspx). These nucleotide changes will subsequently change several amino acids in order to determine their contribution to GABA sensitivity within the *H. contortus* GABA receptor (see Appendix A, Table A1-A4). Introduction of the mutations in the Hco-UNC-49 coding sequence was performed using the QuikChange® Site-Directed Mutagenesis Kit (Stratagene, La Jolla, CA, USA) and verified using DNA sequencing (Genome Quebec). A linearized version of the mutated construct (100-600 ng) was then used as a template in the mMessage mMachine *in vitro* transcription reaction using T7 RNA polymerase provided in a capped RNA transcription kit (Ambion, Austin, TX, USA). Capped *Hco-unc-49* copy RNA (cRNA) was then precipitated using lithium chloride and subsequently resuspended in H_2O at a final concentration of 0.5 ng/nl. Approximately 10–25 μg of cRNA was generated per *in vitro* transcription reaction.

3.2 Expression of Hco-UNC-49 in Xenopus laevis oocytes

Oocytes were surgically removed from *X. laevis* females (Nasco) while anesthetised using 0.15% (w/v) 3-aminobenzoic acid ethyl ester, methane sulphonate salt (MS-222, pH 7; Sigma, Oakville, Ont.), buffered using sodium bicarbonate at pH 7. Harvested oocytes were partitioned into small clusters of less than 20 oocytes and defolliculated using type II collagenase solution (2 mg/mL; Sigma) in OR2 buffer (82 mM NaCl, 2 mM KCl, 1 mM $MgCl_2$, 5 mM Hepes pH 7.5) for 2 hours under light shaking at room temperature. Oocytes were then transferred into ND96 frog saline (96 mM NaCl, 2 mM KCl, 1.8 mM $CaCl_2$, 1 mM $MgCl_2$, 5 mM HEPES) supplemented with 275 µg/ml pyruvate (a carbon source), and gentamycin (100 µg/ml; Sigma). Oocytes were cytoplasmically injected with 50 nl of capped *Hco-unc-49* cRNA (0.5 ng/nl; wild-type and mutants) using the Drummond Nanoject microinjector (Broomhall, PA, USA). Incubation and maintenance of the injected oocytes occurred over a 1- 4 day period at 20°C while submerged in supplemented ND96. Continual replacement of supplemented ND96 occurred approximately every 12 hours. Electrophysiological recordings were performed 2-5 days, post cRNA injections.

3.3 Electrophysiological trials

Two-electrode voltage clamp using microelectrodes was conducted ~ 48 hours, post injection, by means of an Axoclamp 900A voltage clamp (Axon Instruments, Foster City, CA, USA) at 20°C. Standard bath solution and subsequent dose-response recordings were conducted in non-supplemented ND96 frog saline for the duration of the

experiments. Microelectrodes containing Ag|AgCl wires were filled with 3M KCl, upholding a resistance of between 1 – 5 MΩ. The *X. laevis* oocytes were clamped and held at a membrane potential of -60 mV and a subsequent 5 s application of neurotransmitter (at various concentrations, in ND96) was proceeded by a 1-2 min wash with ND96 frog saline. Drugs were washed over the oocytes using an RC-1Z recording chamber (Warner Instrument Inc., Holliston, MA, USA). Data was obtained using Axograph and Clampex 10.0 software (Axon Instruments). Dose–response curves were produced using Graphpad Prism Software 5.0 (San Diego, CA, USA).

3.4 Statistical analysis

Statistical analysis between samples was conducted using a student's t-test where a $p \leq 0.01$ was considered significant (Graphpad Prism Software 5.0). Equations used to generate dose–response curves were fitted to a sigmoidal curve with variable slope. Generation of dose–response curves occurred via fitting obtained data to the following equation:

$$I_{max} = \frac{1}{1 + (EC_{50}/[D])^{h}}$$

Where I_{max} is the maximal response, [D] is the concentration of drug, EC_{50} is the concentration of drug producing a half-maximal effect, and *h* is the Hill coefficient (Forrester *et al.* 2003). The previous equation allows for a sigmoid curve of variable slope to be fitted for normalized data (Forrester *et al.* 2003). Data gathered consisted of at least four independent oocyte recordings for each dose of neurotransmitter. To ensure consistency, mutants were tested over at least two independent batches of oocytes.

3.5 Homology modelling and ligand docking

The protein coding sequence of Hco-UNC-49B (GenBank accession number ACL14329) and Hco-UNC-49C (ABW22635) were aligned with the coding sequence of the AChBP (P58154) using the align2d command in MODELLER 9v7 (Sali and Blundell, 1993) as well as with MacVector v 8.0 (Accelrys, San Diego, USA) and ClustalX v 2.0.12. The crystal structure of the AChBP in the HEPES-bound state at 2.7 Å resolution (Protein Data Bank ID 1I9B) was selected as the template for homology modelling of the Hco-UNC-49 receptor as many other $GABA_A$ receptors, including the related *Drosophila* RDL receptor, have used this template. A three-dimensional model of the extracellular region of the Hco-UNC-49 receptor was constructed using the default parameters in MODELLER through multi-subunit modelling in which one to five subunits were modelled in a single run by repeatedly aligning the template sequence to the desired number of Hco-UNC-49 subunit sequences. A total of 50 models were generated to compensate for low sequence homology. The most energetically favourable models were selected from the MODELLER output file using MODELLIST (http://mordred.bioc.cam.ac.uk/~ricardo/Servers/modellist_s.html) and were subsequently evaluated for violations in stereochemical, volume, and surface properties using PROCHECK (Laskowski *et al.* 1996) and Ramachandran plot analysis (RAMPAGE, http://mordred.bioc.cam.ac.uk/~rapper/rampage.php; Lovell *et al.* 2003). All models were viewed and images generated using UCSF Chimera v 1.4.1 (Pettersen *et al.* 2004). Protonated structural models of GABA were generated using ChemBio3D Ultra 12.0 (CambridgeSoft, Cambridge, U.K.) and were energy minimized using the MM2 force field. Docking of GABA into the Hco-UNC-49 receptor homology model was conducted

using DOCK v 6.4. The binding site of the receptor models were defined using the default parameters in sphgen, grid and dock6 - all accessory programs of DOCK.

Chapter 4 – Results

4.1Template selection for homology modelling

The coding sequence for both Hco-UNC-49B and Hco-UNC-49C were aligned to the coding sequence of the AChBP template (1I9B) to ensure minimal thresholds were met for homology modelling (Figure 5B). ClustalX alignment of Hco-UNC-49B to the template sequence indicated that there was approximately 24% identity and 64% similarity between the sequences. Additionally, Hco-UNC-49C aligned to the template sequence with approximately 28% identity and 66% similarity. To verify 1I9B as a suitable template, the profile.build() command in MODELLER was used. The profile.build() command uses local dynamic algorithms and the target query to identify related sequences from a library of sequences of known protein structures from the Protein Data Bank (Eswar *et al.* 2005). From the resulting output file, the 1I9BA (chain A) template was found to be the top hit for strictly extracellular domain protein templates with an identity score for both Hco-UNC-49B and C of 26% and an E value of 0.1×10^{-2}.

Additionally, the extracellular domains of both Hco-UNC-49 subunits were aligned to the α_1 and β_2 of the $GABA_A$ receptor (Figure 5B). The Hco-UNC-49B had approximately 37% and 42% identity and 69% and 73% similarity to the α_1 and β_2 subunits, respectively. The Hco-UNC-49C had approximately 36% and 40% identity and 70% and 71% similarity to the α_1 and β_2 subunits, respectively. Most of the key amino acids composing the six discontinuous loops associated with ligand binding are conserved across the aligned sequences (Figure 5B). The major sequence differences between the AChBP and the Hco-UNC-49 receptors, with respect to agonist binding structures, occur within loop A and F.

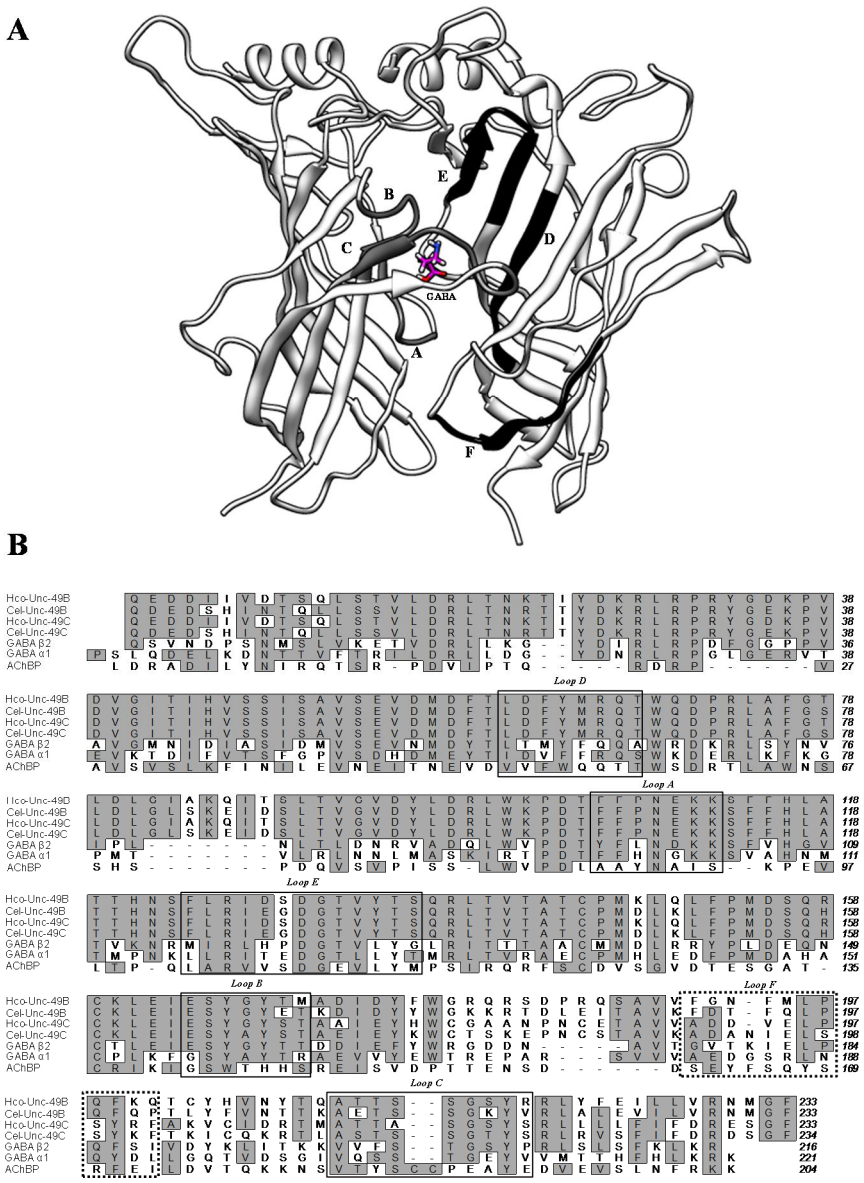

Figure 5. Extracellular domains of the Hco-UNC-49 receptor. A) Model of the Hco-UNC-49B homodimer interface. The binding pocket is formed through the interactions of the six discontinuous loops indicated: Loops A-C (in grey) on the principle subunit and Loops D-F (in black) on the secondary subunit. The GABA molecule can be seen docked near the center of the loops. B) Sequence alignment of the nematode UNC-49 receptor subunits with other receptors from of the Cys-loop superfamily. Identities and similarities between sequences are both shown in dark grey for clarity. Key amino acids which form the loops that are essential to agonist binding are indicated in boxes. A dotted box indicates the sequence of a loop is continued on the next row. Sequences are numbered according to the numbers associated with the Hco-UNC-49 receptor sequences.

4.2 Model selection for homology modelling

The most energetically favourable models, with the lowest structural violations in stereochemical, volume, and surface properties were chosen using MODELLIST and ramachandran plot analysis. Models with the lowest DOPE and molpdf scores were selected and screened on ramachandran plots. DOPE and molpdf scores are values assigned in the MODELLER output file which, when taken together, access the energy of an overall protein in the form of an 'energy score' which sum all the restraint functions. Final models were chosen based on their similarity to the template's associated ramachandran plot, DOPE and molpdf scores. All generated models had no more than 10% of their residues in unfavourable positions on their respective ramachandran plot; a percentage used by PROCHECK which is acceptable for homology models (Hooft *et al.* 1997).

The final extracellular Hco-UNC-49B homodimer structure (Figure 5A) shows a very similar structure to previously modelled vertebrate and invertebrate ionotropic GABA receptors. In addition, the modelling of the UNC-49 and other vertebrate and invertebrate $GABA_A$ subunit monomers revealed similarities in structure and binding loop arrangements (Figure 6). The structure of the homodimer (see Figure 5A) consists of two energetically favourable interacting asymmetric Hco-UNC-49B monomers each with an N-terminal α-helix and 11 β-strands ranging in size from three to 14 amino acids. Due to the interactions of the subunits, the primary subunit has lost a short, three amino acid long 3_{10} helix structure near the N-terminus where each amino acid corresponds to a 120° turn in the right-handed helical structure. This structure is visible on the adjacent subunit.

Additionally, the TM1 would attach to each monomer via the C-terminus located towards the bottom of the each structure immediately after the 11^{th} β-strand.

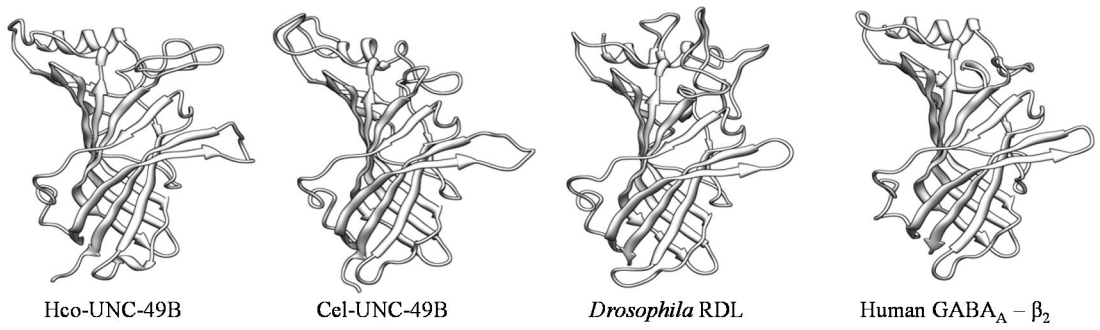

Figure 6. Homology models of various ionotropic GABA receptor monomers. Hco-UNC-49B, Cel-UNC-49B and *Drosophila* RDL represent invertebrate $GABA_A$ receptor subunits. The Cel-UNC-49B monomer was modelled on the AChBP and has not been previously modelled in the literature. The Human $GABA_A - \beta_2$ represents the sole vertebrate $GABA_A$ receptor subunit. For orientation, the N and C termini are located at the 'top' and 'bottom' of each structure, respectively.

The docking of GABA into the binding pocket of the Hco-UNC-49B homodimer interface placed the molecule consistently into the crevice surrounded by Loops B-D (Figure 7); a trend similar to the RDL receptor model (McGonigle and Lummis, 2010). In its most favoured orientation, the carboxyl group of the GABA molecule was positioned adjacent to Arg^{66} of Loop D and to a lesser extent Tyr^{64} of Loop D (Figure 7). The orientation of GABA also placed its ammonium group in close proximity to Tyr^{166} of Loop B as well as Tyr^{218} of Loop C, potentially allowing for ligand-protein cationic-π interactions (Figure 7). Phe^{106} (not a primary focus within this investigation) is an amino acid also located in close proximity to the GABA molecule. A predicted hydrogen-bond between Tyr^{166} and Arg^{66} may align and secure Tyr^{166} in proper orientation for cationic-π bonds with GABA (Figure 7). Thr^{169} is also shown due to its relevance in the current study.

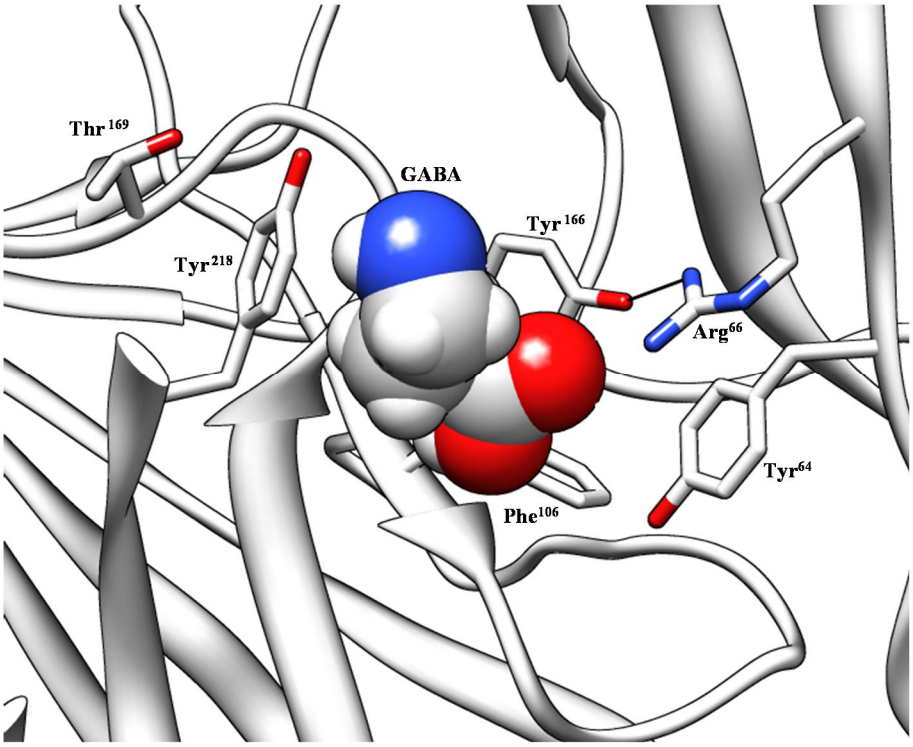

Figure 7. GABA docked within the putative binding pocket of an Hco-UNC-49B homodimer. All amino acids (shown in stick form) predicted to be important in GABA activation are indicated. The ribbon structure of amino acids found in loop C of the primary subunit, that proceed Try^{218}, have been removed for clarity. Amino acids Try^{64}, Phe^{106}, Try^{166} and Try^{218} make up the conserved aromatic box found in other $GABA_A$ receptors. The GABA molecule is shown in space-filling form for ease of viewing. The blue colours represent nitrogen atoms. The red colours represent oxygen atoms.

4.3 Pharmacological characterizations of the Hco-UNC-49 receptors

Heterologous expression of the majority of the mutant *Hco-unc-49B* and *Hco-unc-49C* cRNA in *X. laevis* oocytes formed fully functional GABA-gated channels. Wild-type heteromeric channels produced robust responses (≥3 μA) at 100 μM GABA (Figure 8). Channels with mutations in the Hco-UNC-49B sequence that we found to affect GABA sensitivity also typically produced robust responses (≥3 μA), albeit at higher concentrations compared to the wild-type (Figure 8).

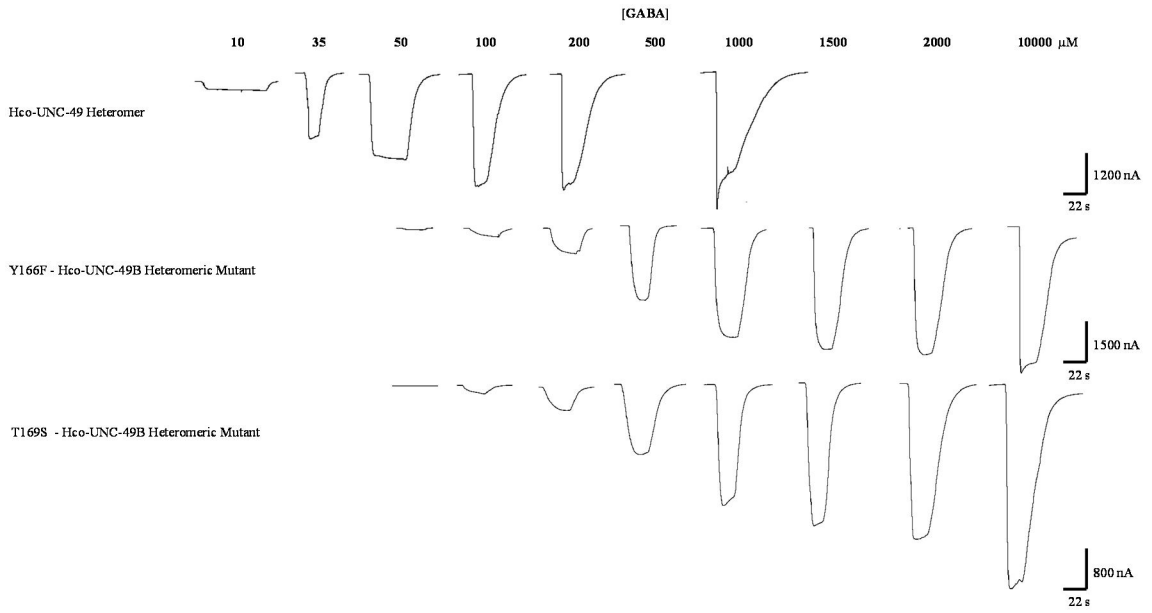

Figure 8. Representative GABA-activated dose-response currents from oocytes expressing wild-type or mutant Hco-UNC-49B channels. GABA concentrations that were applied to the oocytes are indicated at the top.

In general, the wild-type Hco-UNC-49B homomeric channel was slightly less sensitive to GABA (EC_{50}: 63.1 ± 4.2 µM, n = 6; Hill coefficient: 1.7 ± 0.2) compared to its wild-type Hco-UNC-49B/C heteromeric counterpart (EC_{50}: 41.6 ± 4.5 µM, n = 9; Hill coefficient: 1.2 ± 0.1). In most cases, channels with only a single mutated UNC-49B subunit type (i.e. homomeric channels) had a lower sensitivity to GABA compared to channels with a combination of the same mutated UNC-49B subunit with wild-type UNC-49C subunits (i.e. heteromeric channels; see Table 2, 3, and 4).

4.4 Characterization of Loop B in UNC-49B and C subunits

The potential functional differences in Loop B between UNC-49 subunits from *H. contortus* and *C. elegans* were assessed by changing amino acids in the *H. contortus*

Loop B to reflect what is naturally present in Loop B from *C. elegans*. With respect to the UNC-49C subunit, there is only one amino acid difference at position 167 between the two nematodes within BDI of Loop B (see Figure 9). However, mutating $Gly^{167} \rightarrow Ala^{167}$ in Hco-UNC-49C had no effect on GABA sensitivity (Table 2). For the UNC-49B sequences between the two nematode species, there is a difference immediately following BDI (position 170; Figure 9). In addition, there is a difference immediately outside the loop at position 171 (see Figure 9). Of these differences, only the $Met^{170} \rightarrow Thr^{170}$ mutant in the Hco-UNC-49B subunit produced a slight, but statistically significant, decrease in GABA sensitivity in both homo- and heteromeric UNC-49 channels; most notably a two-fold decrease in the UNC-49B/C heteromeric channel (EC_{50}: 88.3 ± 3.3 μM, n = 7; Table 2; Figure 10A-C). To further investigate the importance of position 170 in GABA sensitivity, an additional mutation (M170S) was generated. This mutation had no affect on GABA sensitivity in heteromeric channels. However, the homomeric channel showed an approximate 2.5-fold decrease in GABA sensitivity (EC_{50}: 171.5 ± 12.3 μM, n = 6; Table 2; Figure 10A-C).

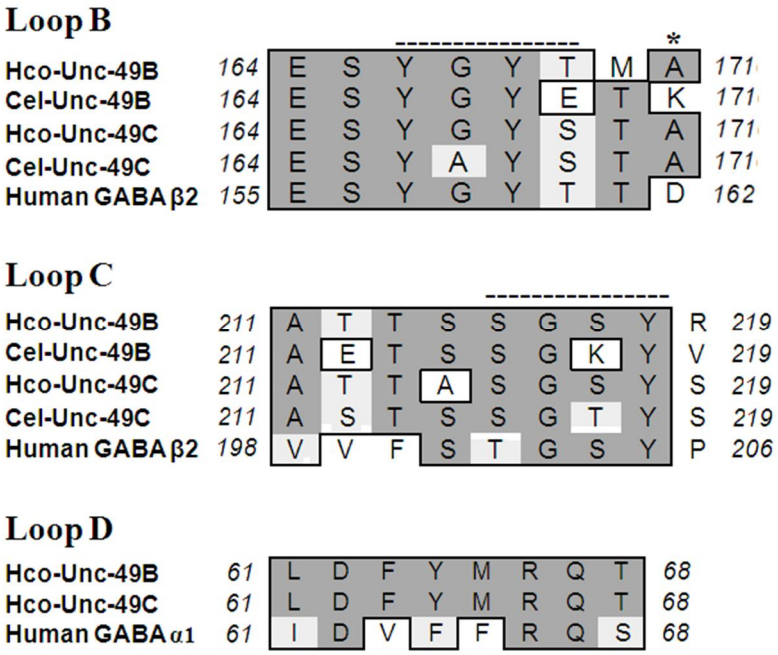

Figure 9. Protein sequence alignment of various loops associated with GABA sensitivity. Dark shaded areas indicate regions of amino acid identity. Light shaded areas indicate regions of amino acid similarity. Non-shaded areas indicate regions of no amino acid similarity. The dash line denotes the amino acids within the putative binding domains (BDI in Loop B; BDII in Loop C). The asterisk above the Loop B alignment indicates that the amino acid is located outside Loop B.

To better understand the role of Loop B in the sensitivity of GABA in nematode UNC-49 receptors, mutations were introduced into the Hco-UNC-49 subunits that were shown to dramatically decrease GABA sensitivity in human $GABA_A$ receptors when the mutations were introduced into the β_2-subunit. Specifically, when Y166F or T169S were introduced into the Hco-UNC-49B subunit, the sensitivity of the heteromeric channels (i.e. mutant Hco-UNC-49B/ wild-type Hco-UNC-49C) to GABA decreased substantially and shifted the EC_{50} to 384.3 ± 49.3 μM (n = 5) and 728.4 ± 75.8 μM (n = 4), respectively (Table 2; Figure 10A-C). The most dramatic effects were seen in the Hco-UNC-49B homomeric channel where the mutations Y166F and T169S decreased GABA sensitivity approximately 9- and 29-fold, respectively (Table 2; Figure 10A-C). An

additional mutation was incorporated at position 166 (Y166S) in Hco-UNC-49B which resulted in heteromeric channels which produced only small responses (≤ 300 nA) to 25 mM GABA and homomeric channels that were unresponsive to GABA at 50 mM (Table 2).

Interestingly, when Y166F was introduced into Hco-UNC-49C, no change in GABA sensitivity was observed (Table 2). It should be noted that a serine is already present at position 169 in Hco-UNC-49C and thus this position was not mutated. All remaining Hco-UNC-49C mutants had no effect on GABA sensitivity (Table 2).

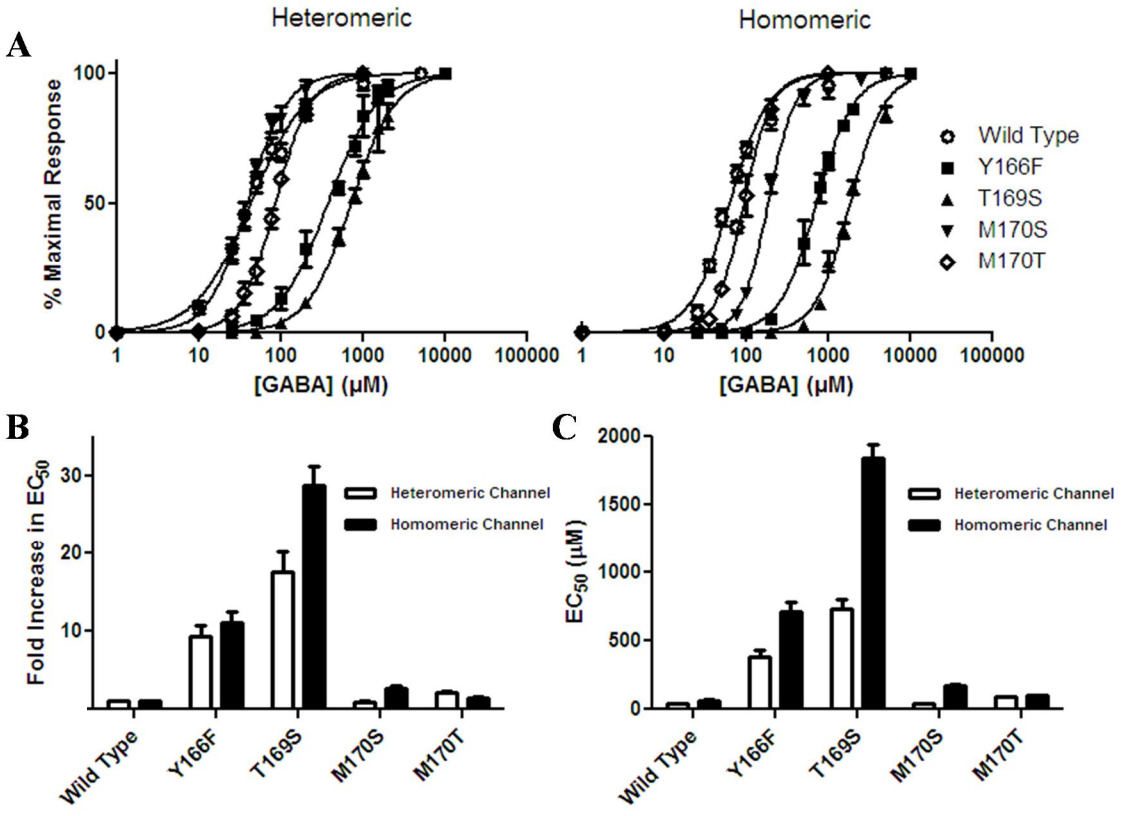

Figure 10. Several Loop B associated mutations affect GABA sensitivity. A) Dose-response curves of wild-type and mutated Hco-UNC-49B receptors. Each data point represents the mean current value ($n \geq 4$ oocytes) normalized to the mean maximum current observed. **Left**: Heteromeric wild-type and mutated Hco-UNC-49B receptors. **Right**: Homomeric wild-type and mutated Hco-UNC-49B receptors. B) Fold increase in EC_{50} of Hco-UNC-49B mutants. C) Comparisons of EC_{50} between heteromeric and homomeric Hco-UNC-49B mutant channels. All error-bars represent standard error of mean (SEM).

Table 2. Comparisons of EC_{50} and Hill coefficient values for wild-type and mutated Loop B Hco-UNC-49 receptors

	Heteromeric[1]		Homomeric	
Mutation[2]	EC_{50} ± S.E. (μM) *(Hill Coefficient* ± S.E.*)*	Number of oocytes	EC_{50} ± S.E. (μM) *(Hill Coefficient* ± S.E.*)*	Number of oocytes
Wild-type	41.6 ± 4.5 *(1.2 ± 0.1)*	9	63.1 ± 4.2 *(1.7 ± 0.2)*	6
UNC-49B				
Y166S	Small responses (≤ 300 nA) at 25 mM	6	No response at 50 mM	6
Y166F	384.3 ± 49.3* *(1.6 ± 0.1)*	5	709.7 ± 69.8* *(2.2 ± 0.3)*	5
T169S	728.4 ± 75.8* *(1.6 ± 0.2)*	4	1838 ± 102.8* *(2.1 ± 0.01)*	4
M170T	88.3 ± 3.3* *(2.3 ± 0.2)*	7	97.0 ± 7.4* *(2.8 ± 0.02)*	9
M170S	39.3 ± 3.6 *(1.8 ± 0.1)*	5	171.5 ± 12.3* *(2.8 ± 0.2)*	6
A171K	42.7 ± 4.6 *(1.7 ± 0.4)*	6	51.7 ± 4.4 *(2.3 ± 0.2)*	7
UNC-49C				
Y166F	49.0 ± 3.8 *(1.2 ± 0.1)*	4	--------	--------
Y167A	32.6 ± 1.8 *(1.7 ± 0.2)*	6	--------	--------

[1] Heteromeric channels are composed of an aforementioned mutant and its wild-type counterpart
[2] Mutants are classified by the amino acid that was changed
All EC_{50} values significantly different from their corresponding wild-type counterpart are denoted by an asterisk (*)

4.5 Homology modelling of the major Loop B mutations

Homology models of the mutants with the largest effect on GABA sensitivity, that remained functional, were generated to visualize the possible affects they have on the structural conformation of the Hco-UNC-49 channels (Figure 11). The most prominent changes occurred within the portions of the loops not found in either α-helices or β-sheets (Figure 11A). Within the Y166F mutant, the orientation of the introduced phenylalanine (shown in blue) is shifted away from the binding pocket and from Try^{218} (shown in orange). In addition, as a result of the switch from Try^{166} to Phe^{166} there is now no hydrogen-bond connecting position 166 to Arg^{66} (Loop D; shown in purple). Furthermore, there is a slight shift of Loop B as well as the introduction of two new hydrogen-bonds which interact with Thr^{169} (shown in red), one of which connects Thr^{169} with Loop C (Figure 11B). In the homology model of mutant T169S (shown in red within Figure 11B), there is a small four amino acid long helical structure (shown in yellow) at the beginning of Loop C that is not present in the wild-type (Figure 11A). In addition, there are some shifts in the binding pocket. For instance, Arg^{66} (shown in purple) is now shifted away from the binding pocket. Additionally, there is also a loss of the predicted hydrogen-bond between Try^{166} (shown in blue) and Arg^{66}.

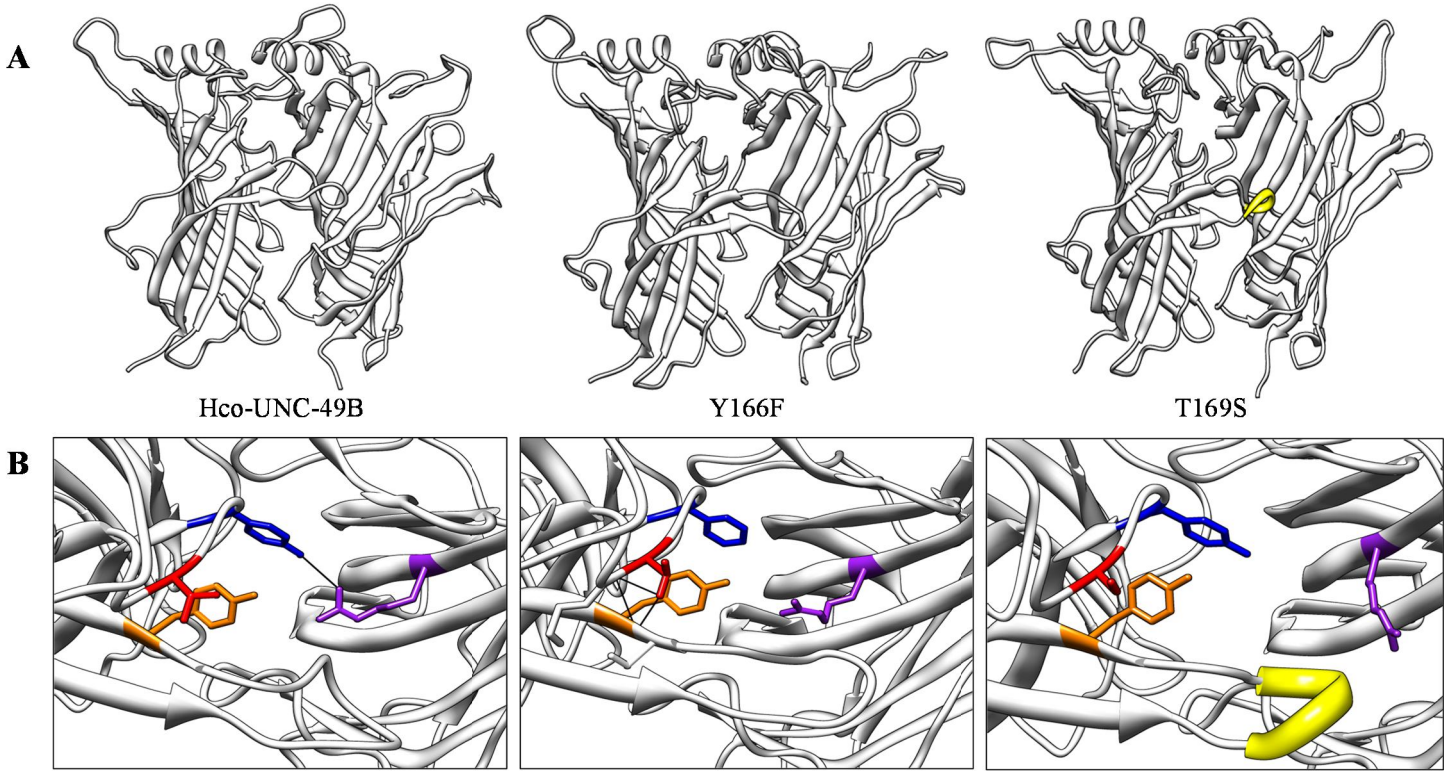

Figure 11. Homology models of the effects of Loop B mutations. A) Hco-UNC-49B wild-type and mutant Loop B homodimer models. The binding pocket is located at the interface of the primary subunit (left) and adjacent subunit (right). B) Close up view of the Hco-UNC-49B wild-type and mutant homodimer binding pocket. Amino acids are identified as follows: position 166 (Loop B; blue), position 169 (Loop B; red), position 218 (Loop C; orange), position 66 (Loop D; purple). Predictive hydrogen-bonds connecting interacting amino acids are indicated as black lines. The four amino acid long helical structure associated with the T169S mutation is shown in yellow.

4.6 Characterization of Loop C in UNC-49B and C subunits

Between the *H. contortus* and *C. elegans* UNC-49C sequences, there are three amino acid differences in Loop C (Figure 9). However, only one difference is located within BDII (Figure 9). Mutational analysis demonstrated that neither A214S nor S217T had any effect on GABA sensitivity when introduced in Hco-UNC-49C (Table 3). The UNC-49B sequences between the two nematode species have only two differences within Loop C, one of which is located within BDII at position 217 (Figure 9). The mutagenesis of $Ser^{217} \rightarrow Lys^{217}$ in the Hco-UNC-49B subunit resulted in no change in GABA sensitivity in either the homo- or heteromeric receptor forms (Table 3).

Two mutations were introduced into Loop C of both Hco-UNC-49B and Hco-UNC-49C subunits at positions that were previously shown to disrupt GABA sensitivity in human $GABA_A$ receptors (T202S and Y205F). However, in Hco-UNC-49B, a serine is already present at the 202 equivalent (Ser^{215}). Therefore, this position was mutated back to a threonine (i.e. $Ser^{215} \rightarrow Thr^{215}$). However, no affect on GABA sensitivity was observed in either the homomeric or heteromeric channels. Only Y218F (205 equivalent) in the Hco-UNC-49B subunit significantly decreased GABA sensitivity (Figure 12A). Within the mutant Hco-UNC-49B heteromeric channel (i.e. mutant Hco-UNC-49B/ wild-type Hco-UNC-49C), the Y218F mutation resulted in a shift in the channels EC_{50} to 697.6 ± 193.8 μM (n = 4); a decrease in GABA sensitivity of approximately 17-fold (Table 3; Figure 12A-C). As a homomeric channel, the Y218F mutation also resulted in a decreased GABA sensitivity lowering the channels EC_{50} to 654.3 ± 41.3 μM (n = 4) (Table 3; Figure 12A-C). Due to the slight difference in EC_{50} between the homo- and heteromeric channel, there is a possibility that the mutated UNC-49B subunit cannot

assemble with UNC-49C. To confirm the formation of heteromeric channels, the mutant Y218F channels were tested with the GABA receptor antagonist PTX (Figure 12D). Similar to previous reports (Siddiqui *et al.* 2010), there was almost complete inhibition within the mutant homomeric channel, but when mutated UNC-49B was co-expressed with wild-type UNC-49C, the resulting channel became PTX resistant (Figure 12D) indicating that the UNC-49B/C subunits were in fact co-assembled. Interestingly, when the Y218F mutation was introduced into Hco-UNC-49C, it had no affect on GABA sensitivity (Table 3).

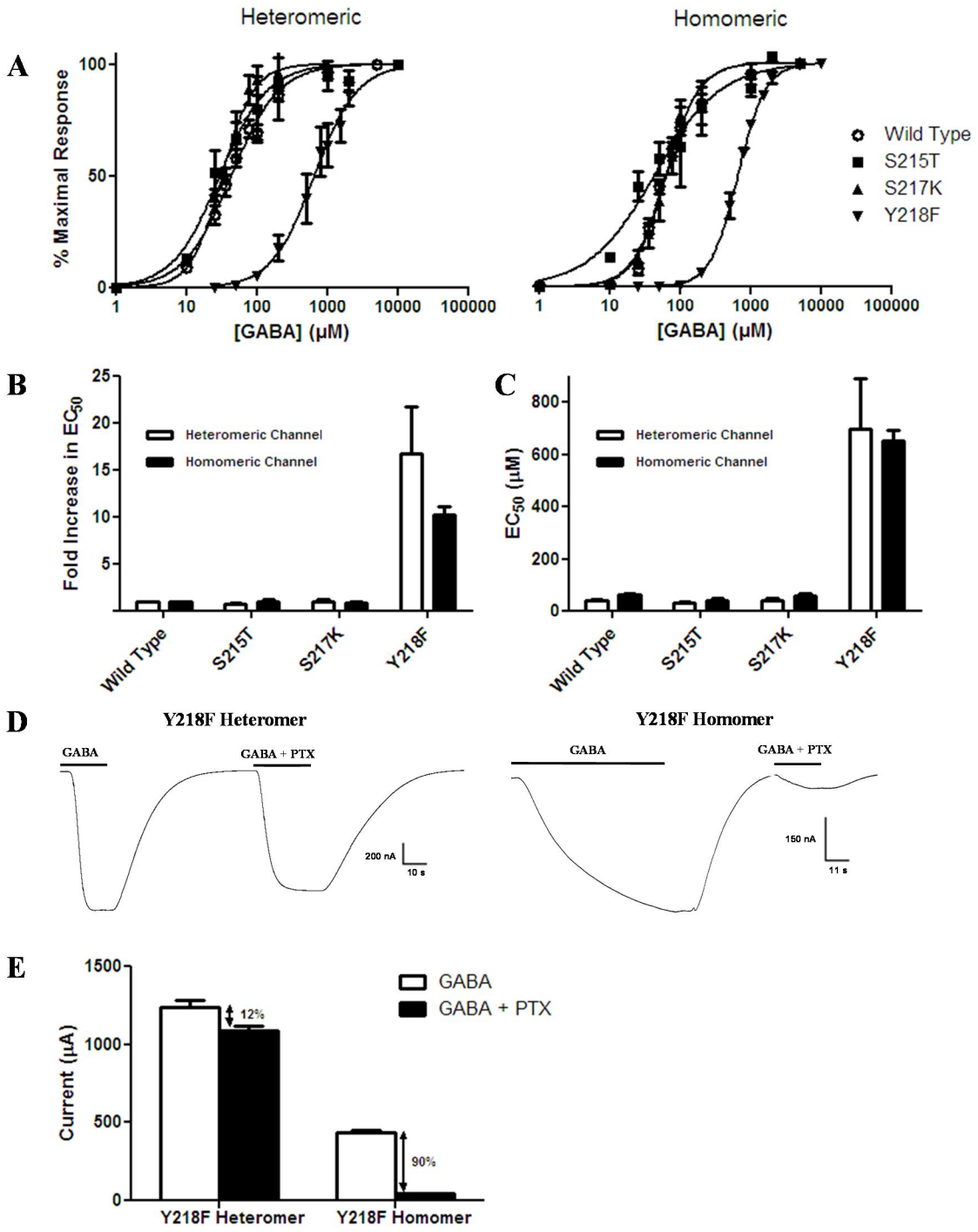

Figure 12. One Loop C associated mutation lowers GABA sensitivity. A) Dose-response curves of wild-type and mutated Hco-UNC-49B receptors. Each data point represents the mean current value ($n \geq 4$ oocytes) normalized to the mean maximum current. **Left**: Heteromeric wild-type and mutated Hco-UNC-49B receptors. **Right**: Homomeric wild-type and mutated Hco-UNC-49B receptors. B) Fold increase in EC_{50} of Hco-UNC-49B mutants. C) Comparisons of EC_{50} between heteromeric and homomeric Hco-UNC-49B mutant channels. D) Hco-UNC-49B mutant Y218F heteromeric channels are more resistant to PTX inhibition compared to Y218F mutant homomeric channels. Receptors were initially hit with 700 μM GABA proceeded by 700 μM GABA combined with 100 μM PTX. E) The percent PTX-dependent inhibition of the GABA responses for each channel. All error-bars represent standard error of mean (SEM).

Table 3. Comparisons of EC_{50} and Hill coefficient values for wild-type and mutated Loop C Hco-UNC-49 receptors

Mutation[2]	Heteromeric[1]		Homomeric	
	EC_{50} ± S.E. (μM) *(Hill Coefficient* ± S.E.*)*	Number of oocytes	EC_{50} ± S.E. (μM) *(Hill Coefficient* ± S.E.*)*	Number of oocytes
Wild-type	41.6 ± 4.5 *(1.2 ± 0.1)*	9	63.1 ± 4.2 *(1.7 ± 0.2)*	6
UNC-49B				
S215T	34.3 ± 4.2 *(1.3 ± 0.2)*	6	43.2 ± 6.7 *(1.1 ± 0.1)*	6
S217K	42.5 ± 7.6 *(1.9 ± 0.2)*	13	58.9 ± 8.5 *(2.6 ± 2.2)*	12
Y218F	697.6 ± 193.8* *(1.6 ± 0.1)*	4	654.3 ± 41.3* *(2.3 ± 0.3)*	4
UNC-49C				
A214S	31.6 ± 1.9 *(1.3 ± 0.1)*	13	--------	--------
S215T	35.6 ± 2.1 *(1.9 ± 0.1)*	4	--------	--------
S217T	34.6 ± 3.1 *(1.4 ± 0.1)*	14	--------	--------
Y218F	53.9 ± 3.0 *(1.9 ± 0.01)*	4	--------	--------

[1] Heteromeric channels are composed of an aforementioned mutant and its wild-type counterpart
[2] Mutants are classified by the amino acid that was changed
All EC_{50} values significantly different from their corresponding wild-type counterpart are denoted by an asterisk (*)

4.7 Homology modelling of the major Loop C mutations

Similar to the Loop B homology models, the most disruptive changes to structure were observed in non-secondary structure configurations (Figure 13A). In the model for Y218F (shown in orange within Figure 13B), Ser^{217} (shown in green) now has no predicted hydrogen-bonds associated with it, whereas Ser^{217} in the wild-type homodimer

has one associated hydrogen-bond (Figure 13B). In addition, Loop C in the Y218F homology model forms a more relaxed structure, in relation to the wild-type homodimer (Figure 13A and B). Furthermore, there are subtle differences in protein structure throughout the mutant model with respect to the wild-type model. Additionally, Arg^{66} (in Loop D; shown in purple) is shifted away from the binding pocket and the predicted hydrogen-bond between Try^{166} (in Loop B; shown in blue) and Arg^{66} is not present which may possibly destabilize the architecture of the binding pocket (Figure 13B).

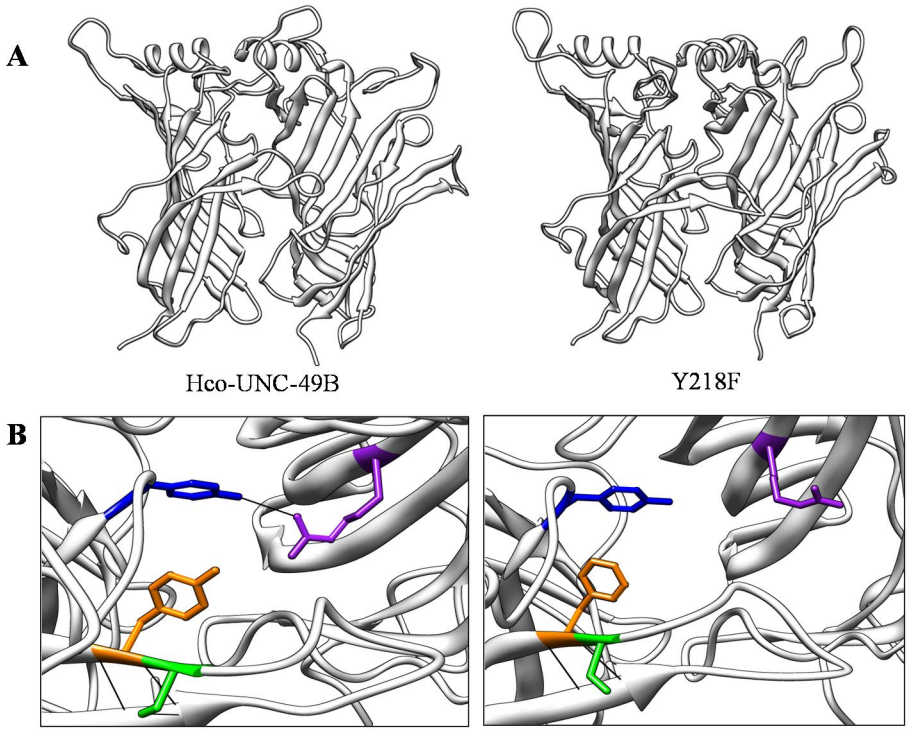

Figure 13. The effect of Loop C mutation Y218F. A) Hco-UNC-49B wild-type and mutant Loop C homodimer models. The binding pocket is located at the interface of the primary subunit (left) and adjacent subunit (right) B) Close up view of the Hco-UNC-49B homodimer binding pocket in the wild-type and Y218F mutant receptor. Amino acids are identified as follows: position 166 (Loop B; blue), position 217 (Loop C; green), position 218 (Loop C; orange) and position 66 (Loop D; purple). Predictive hydrogen-bonds connecting interacting amino acids are indicated as black lines.

4.8 The effect of Loop D mutations on Hco-UNC-49 subunits

Based on the model of the UNC-49 channel binding pocket, as well as other research on mammalian $GABA_A$ receptors, Loop D is found on the adjacent subunit. In the mammalian $GABA_A$ receptor binding pocket, the α-subunit donates Loops D-F to GABA binding. However, when aligned with the α-subunit, the Hco-UNC-49 subunits do not have a high degree of sequence similarity (Figure 9). Nonetheless, Try^{64} in both Hco-UNC-49 sequences appear to be equivalent to Phe^{64} in the α-subunit (Figure 9); an amino acid shown to be essential to GABA sensitivity in mammalian $GABA_A$ receptors when mutated to a leucine (Sigel *et al.* 1992). When the $Try^{64} \rightarrow Leu^{64}$ mutant was introduced into Hco-UNC-49B, it had a profound effect on GABA sensitivity, decreasing the sensitivity of the heteromeric channel to GABA by roughly 19-fold (EC_{50} to 804.3 ± 104.9 μM, n = 7) and the homomeric channel by roughly 194-fold (EC_{50} to 12 425 ± 849.7 μM, n = 8; Table 4; Figure 14A-C). Leucine substitutions were also conducted on amino acids at the adjacent positions, 63 and 65, in the Hco-UNC-49B subunit. These mutants produced small differences in GABA sensitivity in the homomeric channel (Table 4; Figure 14A-C). Consistent with previous loops analyzed in this study, the same mutations introduced into Hco-UNC-49C did not affect GABA sensitivity (Table 4).

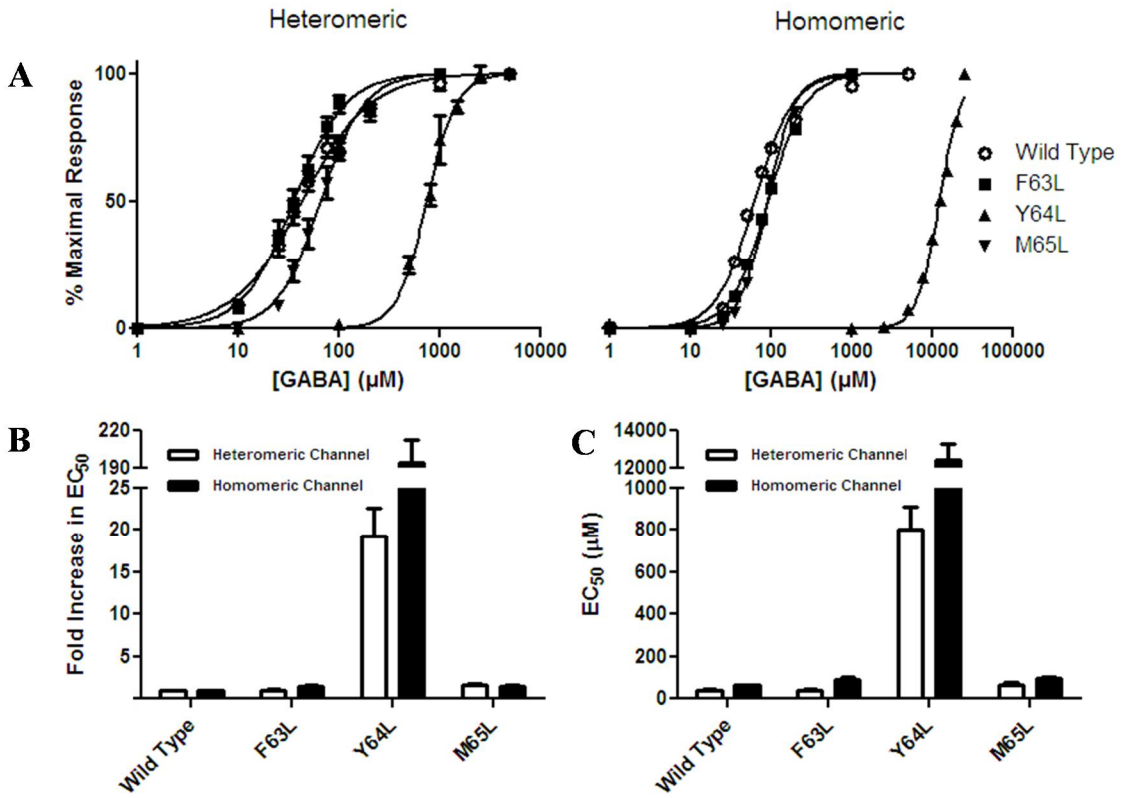

Figure 14. One Loop D associated mutation lowers GABA sensitivity. A) Dose-response curves of wild-type and mutated Hco-UNC-49B receptors. Each data point represents the mean current value ($n \geq 4$ oocytes) normalized to the mean maximum current. **Left**: Heteromeric wild-type and mutated Hco-UNC-49B receptors. **Right**: Homomeric wild-type and mutated Hco-UNC-49B receptors. B) Fold increase in EC_{50} of Hco-UNC-49B mutants. C) Comparisons of EC_{50} between heteromeric and homomeric Hco-UNC-49B mutant channels. All error-bars represent standard error of mean (SEM).

Table 4. Comparisons of EC_{50} and Hill coefficient values for wild-type and mutated Loop D Hco-UNC-49 receptors

Mutation[2]	Heteromeric[1]		Homomeric	
	EC_{50} ± S.E. (μM) *(Hill Coefficient* ± S.E.*)*	Number of oocytes	EC_{50} ± S.E. (μM) *(Hill Coefficient* ± S.E.*)*	Number of oocytes
Wild-type	41.6 ± 4.5 *(1.2 ± 0.1)*	9	63.1 ± 4.2 *(1.7 ± 0.2)*	6
UNC-49B				
F63L	37.9 ± 5.6 *(1.9 ± 0.2)*	7	93.2 ± 10.3* *(2.2 ± 0.4)*	5
Y64L	804. 3 ± 104.9* *(2.0 ± 0.3)*	7	12 425 ± 849.7* *(3.5 ± 0.3)*	8
M65L	67.7 ± 8.4 *(2.1 ± 0.06)*	6	94.7 ± 10.0* *(2.7 ± 0.4)*	5
UNC-49C				
F63L	30.6 ± 0.8 *(1.7 ± 0.1)*	5	--------	--------
Y64L	61.3 ± 8.2 *(2.1 ± 0.4)*	9	--------	--------
M65L	51.3 ± 8.8 *(1.3 ± 0.2)*	6	--------	--------

[1] Heteromeric channels are composed of an aforementioned mutant and its wild-type counterpart
[2] Mutants are classified by the amino acid that was changed
All EC_{50} values significantly different from their corresponding wild-type counterpart are denoted by an asterisk (*)

4.9 Homology modelling of the major Loop D mutations

Similar to the Loop B and C homology models, the most considerable changes to structure are seen within non-secondary structural arrangements (Figure 15A). In the Y64L homology model, the mutation of $Try^{64} \rightarrow Leu^{64}$ (shown in magenta) removes the aromatic tyrosine residue from the binding pocket (Figure 15B). Additionally, Arg^{66} (shown in purple) now forms two intra-loop hydrogen-bonds with Thr^{68} (shown in cyan;

Figure 15B). Furthermore, Arg[66] is completely removed from the binding pocket and does not form the predicted hydrogen-bond with Tyr[166] (shown in blue; Figure 15B).

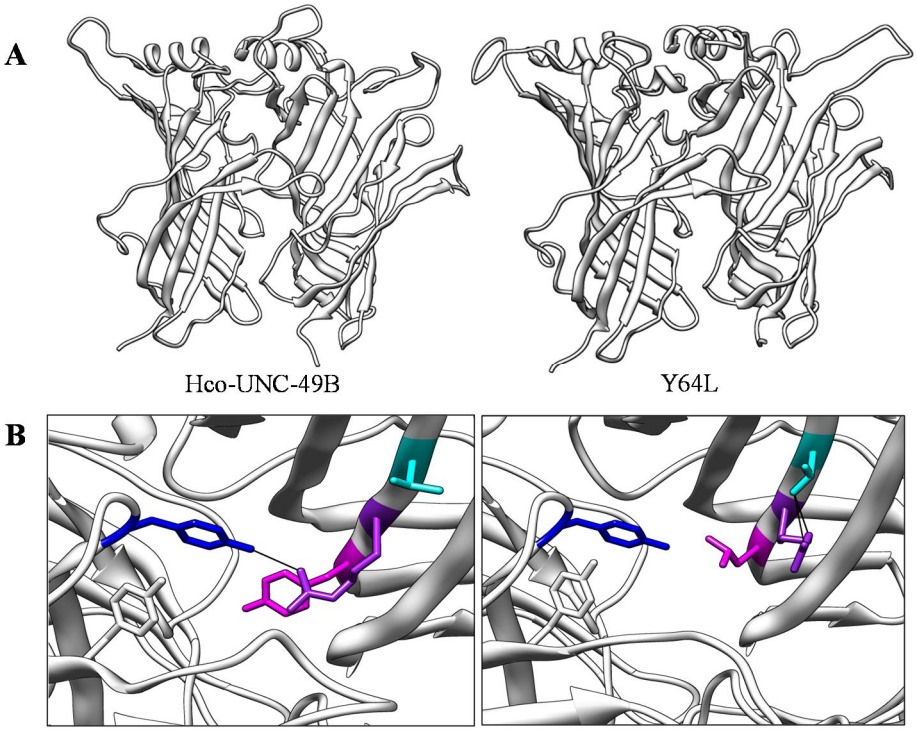

Figure 15. The effect of Hco-UNC-49B Loop D mutation Y64L. A) Hco-UNC-49B wild-type and mutant Loop D homodimer models. The binding pocket is located at the interface of the primary subunit (left) and adjacent subunit (right) B) Close up view of the Hco-UNC-49B homodimer binding pocket. Amino acids are identified as follows: position 166 (Loop B; blue), position 64 (Loop D; magenta), position 66 (Loop D; purple), position 68 (Loop D; cyan). Predictive hydrogen-bonds connecting interacting amino acids are indicated as black lines. Try[218] is shown in white to indicate the location of Loop C.

4.10 Homomeric channels typically have higher Hill coefficients compared to heteromeric channels

Homomeric channels were shown to typically possess higher Hill coefficients than heteromeric channels (Figure 16). Although several mutations caused the UNC-49 channels to require more GABA for channel activation, there were no significant changes

in desensitization kinetics as all mutants recovered from GABA activation similarly to their wild-type counterparts.

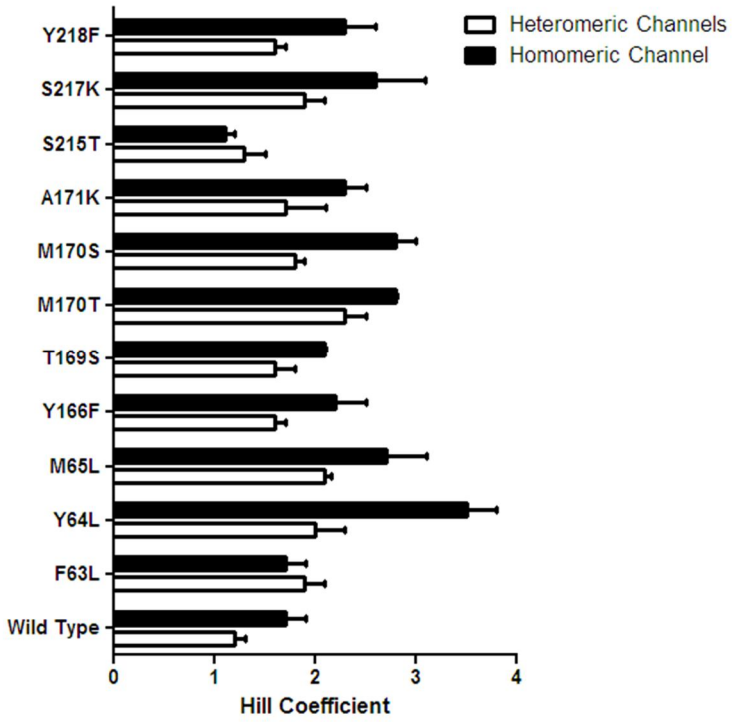

Figure 16. Hill coefficients for mutant Hco-UNC-49B channels. All the bars represent either a homomeric or heteromeric mutated Hco-UNC-49B receptor. Each bar represents the mean Hill coefficient ($n \geq 4$ oocytes). Error-bars represent standard error of mean (SEM).

Chapter 5 – Discussion

5.1 Equivalent amino acid positions play analogous roles in invertebrate and vertebrate $GABA_A$ receptors

Most of our understanding of the Cys-loop receptor agonist binding has been developed through work with the nAChR (Cromer *et al.* 2002). Nonetheless, methods such as amino acid mutagenesis and photo-affinity labelling have been fundamental in advancing our understanding of the essential elements involved in $GABA_A$ receptor activation (Sigel *et al.* 1992; Amin and Weiss, 1993; Smith and Olsen, 1994; Boileau *et al.* 2002; Padgett *et al.* 2007). Unfortunately, there is currently a gap in our understanding regarding the molecular characterization of the determinants important for agonist activation of invertebrate Cys-loop receptors which have been demonstrated to be important targets for both insecticides and anthelmintics (Casida, 1993; Casida, 2009). This thesis has attempted to bridge this gap and represents, to our knowledge, the first investigation of molecular determinants important for the activation of an invertebrate $GABA_A$ receptor by its natural agonist.

Cys-loop receptor subunits appear to have a high degree of structural similarity particularly within the architecture of their extracellular or 'ligand-binding' domain (Ernst *et al.* 2005). This is especially true when one observes the architectural conservation within the binding loops of these receptors. The homology models generated for the Hco-UNC-49 subunits produced the characteristic six discontinuous loops (Loops A-F) associated with binding in roughly the same orientation and location as other Cys-loop receptors such as the nAChR, 5-HT_3, $GABA_A$, $GABA_C$ and the *Drosophila* RDL receptor (Boileau *et al.* 2002; Karlin, 2002; Ernst *et al.* 2005, Harrison and Lummis, 2006; Thompson and Lummis, 2007; McGonigle and Lummis, 2010). This is not surprising as even proteins with low amino acid sequence homology may still form

similar structural and functional domains (Murzin, 1998). However, in our case there is a relatively high degree of amino acid similarity between the Loops A-E of the Hco-UNC-49 subunits and the α- and β-subunits of the vertebrate $GABA_A$ receptor. This suggests that the structural determinates important for GABA activation in invertebrates and vertebrates are similar.

The role of these loops, particularly B, C and D (the focus of this study), in the function of the Hco-UNC-49 channel were investigated through site directed mutagenesis and homology modelling. Overall, results from this study determined that the majority of amino acids shown to be essential for GABA sensitivity within the vertebrate $GABA_A$ receptor also had analogous roles in the Hco-UNC-49 receptor. For instance, previous data has implicated β_2Thr^{160} (in Loop B) as essential for vertebrate GABA receptor activation (Amin and Weiss, 1993). Similarly, when the Hco-UNC-49 equivalent position (Thr^{169}) was mutated to a serine it also caused a dramatic decrease in GABA sensitivity suggesting that both vertebrate and invertebrate $GABA_A$ receptors require this conserved threonine within Loop B. While homology modelling suggests that Thr^{169} may not be in direct contact with GABA (Figure 7), its change to a serine appears to result in significant structural changes in the binding site which may explain the altered sensitivity of the channel to GABA.

In the vertebrate $GABA_A$ receptor, it has been shown that four aromatic residues are essential for binding; forming what is commonly referred to as an 'aromatic box' located on the inter-subunit interface between Loops A-D of two dissimilar subunits (Padgett *et al.* 2007; Pless *et al.* 2008). In fact, many Cys-loop receptors (the nAChR, the $5\text{-}HT_3$ receptor, and the *C. elegans* 5-HT-gated Cl^- channel, MOD-1) possess a conserved

'aromatic box' indicating its importance in agonist binding (Lester *et al.* 2004; Pless *et al.* 2008). Homology modelling of the Hco-UNC-49 receptor has also shown the presence of a putative 'aromatic box' (Figure 7) suggesting that this region is also important for GABA binding in invertebrate receptors.

Within the vertebrate $GABA_A$ receptor, four amino acids (α_1Phe^{64}, Loop D; β_2Try^{97}, Loop A; β_2Try^{157}, Loop B; β_2Try^{205}, Loop C) form the aromatic box with β_2Try^{97} participating in cationic-π interactions with the ammonium of the GABA molecule and $\beta_2Try^{157}$and β_2Try^{205} interacting with the carboxyl group of GABA (Padgett *et al.* 2007). The roles of $Try^{157}$and Try^{205} have been thoroughly investigated in the $GABA_A$ receptor and both have been shown, when mutated to phenylalanine, to dramatically decrease GABA sensitivity (Amin and Weiss, 1993). In this study, similar effects were observed when the same mutations were introduced into the equivalent $Try^{166}$and Try^{218} positions of the Hco-UNC-49B subunit indicating that these amino acids play analogous roles in the UNC-49 receptor. Indeed, both amino acids are positioned in close proximity to GABA when docked (Figure 7) and likely contribute to an aromatic box in the Hco-UNC-49 receptor. In addition, it has been speculated that residue Try^{157} (Try^{166} equivalent) plays a role in the hydrogen-bond network within the binding pocket of the vertebrate $GABA_A$ receptor forming a hydrogen-bond with the -NH of the α_1Thr^{130} backbone (Padgett *et al.* 2007). This bond is thought to stabilize the binding pocket allowing β_2Tyr^{97} to form a cation–π interaction with GABA (Padgett *et al.* 2007). This arrangement is consistent with a high majority of Cys-loop receptors which have aromatic residues located on either Loop B (nACh, $5\text{-}HT_3$ and $GABA_C$ receptors) or Loop C (MOD-1 receptors) which form cation-π interactions with the ligand (Pless *et al.*

2008). Homology modelling of the Hco-UNC-49 receptor indicates a similar function of Try^{166} which appears to form a stabilizing hydrogen-bond with Arg^{66} (Figure 7) which may be important for overall structure of the binding site and the positioning of key amino acid residues that interact with GABA. It is interesting to note that in the homology models of all the mutations that had a substantial affect on GABA sensitivity, the hydrogen-bond between Try^{166} and Arg^{66} was lost. Finally, the importance of the Try^{166} is further illustrated by the finding that when the mammalian equivalent was mutated into a serine, there was a near 1000-fold reduction in GABA sensitivity (Amin and Weiss, 1993). Consistent with this, when we mutated position 166 to a serine in Hco-UNC-49B, there was only a small response ($\leq$ 300 nA) to very high concentrations of GABA (>25 mM) in the heteromeric channel and no current was observed using up to 50 mM GABA in the homomeric channel. This further suggests a conserved role for this position in nematode GABA receptors.

A notable difference between Hco-UNC-49 and vertebrate $GABA_A$ receptors is the role of Thr^{202} (vertebrate) and Ser^{215} (Hco-UNC-49 equivalent). Previous data suggests that when Thr^{202} in the vertebrate $GABA_A$ receptor is mutated to a serine, GABA sensitivity was decreased approximately 21–fold (Amin and Weiss, 1993). However, both Hco-UNC-49 subunits (B and C) possess a serine in the equivalent position. To examine this position further, Ser^{215} was mutated to Thr^{215} which resulted in no change in GABA sensitivity. Interestingly, in the Hco-UNC-49 homology model between receptors with either a Ser^{215} or Thr^{215} there were only minute differences (data not shown). On the other hand, the $Thr^{202} \rightarrow Ser^{202}$ vertebrate $GABA_A$ receptor mutant model (i.e. β_2-α_1 dimer) produced drastic changes in both shape and orientation of Loop

A. These changes resulted in the upward 'kinking' of Loop A allowing the formation of new predicted hydrogen-bonds between Loop A of the β_2-subunit and the amino acids just prior to Loop E on the α_1-subunit (data not shown). Thus it appears that position 202 in the vertebrate $GABA_A$ receptor may be critical for the overall structural conformation of the binding pocket rather than directly interacting with the GABA molecule itself. In fact, research by other groups has revealed that Thr^{202} may not make direct contact with GABA in the binding pocket (Wagner and Czajowski, 2001). It is clear, however, that this position is important for channel function in vertebrate GABA receptors, but possibly not as much in Hco-UNC-49.

Another interesting observation was that while positions 166 and 218 in the UNC-49 receptor appear to have analogous roles to the mammalian $GABA_A$ receptor, the mutations in the UNC-49 channel (specifically the heteromeric channel) had a less drastic affect on GABA sensitivity compared to what was previously observed for the mammalian channel (Amin and Weiss, 1993). These differences may be the result of our particular perfusion system and experimental setup. However, it is more likely that there are in fact inherent differences in the structure of the binding pocket between nematode and mammalian $GABA_A$ receptors. Further research would be required to determine the exact structural differences important for GABA binding and activation in nematode verses mammalian receptors.

5.2 One amino acid may partially account for differences in GABA sensitivity between nematode UNC-49 receptors

Previous research by our group demonstrated that the Hco-UNC-49B/C heteromeric channel was approximately 2.5-fold more sensitive to GABA than that of the

Cel-UNC-49B/C receptor (Siddiqui *et al.* 2010). The apparent increased sensitivity appears to be linked to the Hco-UNC-49B subunit (Siddiqui *et al.* 2010). Examination of Loop B and C identified several key amino acids that were variable between the *H. contortus* and *C. elegans* UNC-49B subunits. However, of all the positions that were different between the two nematodes, the only mutations that had any noticeable affect were those introduced at position 170 of Loop B. In *H. contortus* a Met^{170} is present while *C. elegans* exhibits a threonine at the equivalent position. The mutation M170T resulted in an approximate 2-fold decrease in GABA sensitivity in the heteromeric channel. The importance of position 170 was also verified by introducing an additional mutation (M170S) which caused a 2.5-fold decrease in GABA sensitivity in the homomeric channel. Interestingly, in the $GABA_A$ receptor β_2-subunit, a mutation from threonine to arginine in the equivalent position (Thr^{161}) altered GABA sensitivity by almost 3-fold (Amin and Weiss, 1993). Therefore, it appears that this position may play a small role in GABA activation in both vertebrate and UNC-49 receptors and may partially account for the difference in GABA sensitivity between *H. contortus* and *C. elegans* channels.

5.3 The binding site of Hco-UNC-49 is located between similar subunits

UNC-49 receptors have been identified in many free-living nematodes such as *C. elegans* (Bamber *et al.* 1999), *C. briggsae*, *C. brenneri*, *C. japonica* and *C. remanei* (Wormbase) as well as in the parasitic nematode *H. contortus* (Siddiqui *et al.* 2010). Their presence in a wide variety of nematode species may be indicative of their importance to nematode GABAergic systems. In *C. elegans*, the UNC-49 receptors are

expressed at the neuromuscular junction where the co-assembly of two subunits (UNC-49B and UNC-49C) results in the formation of a heteromeric GABA receptor which has been demonstrated to act as the neuromuscular $GABA_A$ receptor *in vivo* (Bamber *et al.* 1999; Bamber *et al.* 2003; Bamber *et al.* 2005).

The significance of Cel-UNC-49C in heteromeric channels is quite evident as its co-assembly with Cel-UNC-49B confers PTX resistance, a decrease in GABA sensitivity and changes in desensitization kinetics (Bamber *et al.* 1999; Bamber *et al.* 2003; Bamber *et al.* 2005). In *H. contortus*, Hco-UNC-49C exerts its influence by increasing GABA sensitivity in heteromeric channels while simultaneously causing the channels to become PTX resistant (Siddiqui *et al.* 2010). The characterization of native GABA receptors in the muscle cells of the parasitic nematode *Ascaris suum* have shown these receptors possess similar pharmacological properties to those observed for the UNC-49B/C heteromeric channel (Holden-Dye *et al.* 1989; Walker *et al.* 1992; Martin, 1993, Bamber *et al.* 2003). Thus, it appears as though the formation of heteromeric UNC-49-like channels *in vivo* is conserved and functionally important in nematodes (Bamber *et al.* 2003). However, what is not known is whether UNC-49C exerts a direct or indirect effect on GABA binding and channel activation.

Within vertebrate $GABA_A$ receptors, the GABA binding site is located at the interface of two dissimilar subunits: the primary β–subunit and the secondary, or adjacent, α–subunit (Lummis, 2009). However, it is not known whether the UNC-49C subunit contributes to the binding-site interface in UNC-49 receptors. To begin to address this question, mutations in Loops B and C were introduced into the Hco-UNC-49C subunit which included mutations at positions shown to dramatically affect GABA

sensitivity when introduced in Hco-UNC-49B (positions 166 and 218). However, none of the Hco-UNC-49C mutations produced a noticeable effect on GABA sensitivity in the heteromeric channels. Furthermore, in vertebrate $GABA_A$ receptors, the mutation of α_1Phe^{64} (found in Loop D on the adjacent subunit) to Leu^{64} caused a dramatic decrease in GABA sensitivity by roughly 200-fold (Sigel *et al.* 1992). Intriguingly, when the same mutation was introduced into the Hco-UNC-49C equivalent, Try^{64}, no change in GABA sensitivity was observed. However, when the same mutation was introduced into Hco-UNC-49B, a significant reduction in GABA sensitivity was observed.

Taken together, these results suggest two possibilities about the nature of the UNC-49 binding site. First, there is a binding site on the UNC-49B-C interface, but other residues on the UNC-49C subunit (not examined in this study) contribute directly to GABA binding and channel activation. Second, the binding site is on the UNC-49B-B interface and UNC-49C plays an indirect role in the sensitivity of the channel to GABA. The latter scenario seems more likely since UNC-49B homomeric channels with functional agonist binding sites are readily formed in oocytes. In addition, in *C. elegans* only UNC-49B is essential for receptor function (Bamber *et al.* 1999). Interestingly, in most cases, the Hill slopes for homomeric channels are higher than the heteromeric channels, suggesting that a channel with five UNC-49B subunits requires more molecules of GABA to activate the channel compared to a channel with a combination of UNC-49B and C subunits (Weiss, 1997).

If Hco-UNC-49C does not play a direct role in GABA binding, then what is the function of this subunit? As stated previously, UNC-49C likely indirectly modulates the sensitivity and the overall kinetics of the channel. Indeed, the introduction of Hco-UNC-

49C increases the sensitivity of the majority of the channels examined in this study. Therefore, the assembly of the Hco-UNC-49C with Hco-UNC-49B subunits may influence the conformation of the channel which in turn alters either the binding site so that GABA binds at a higher affinity or produces a more sensitive channel. However, further research is required to determine the exact changes that occur in the channel when assembled as a homomer or heteromer. For illustrative purposes, a model of an Hco-UNC-49B homomeric channel and a hypothetical Hco-UNC-49B/C heteromeric channel with indicated binding site regions can be found below (see Figure 17).

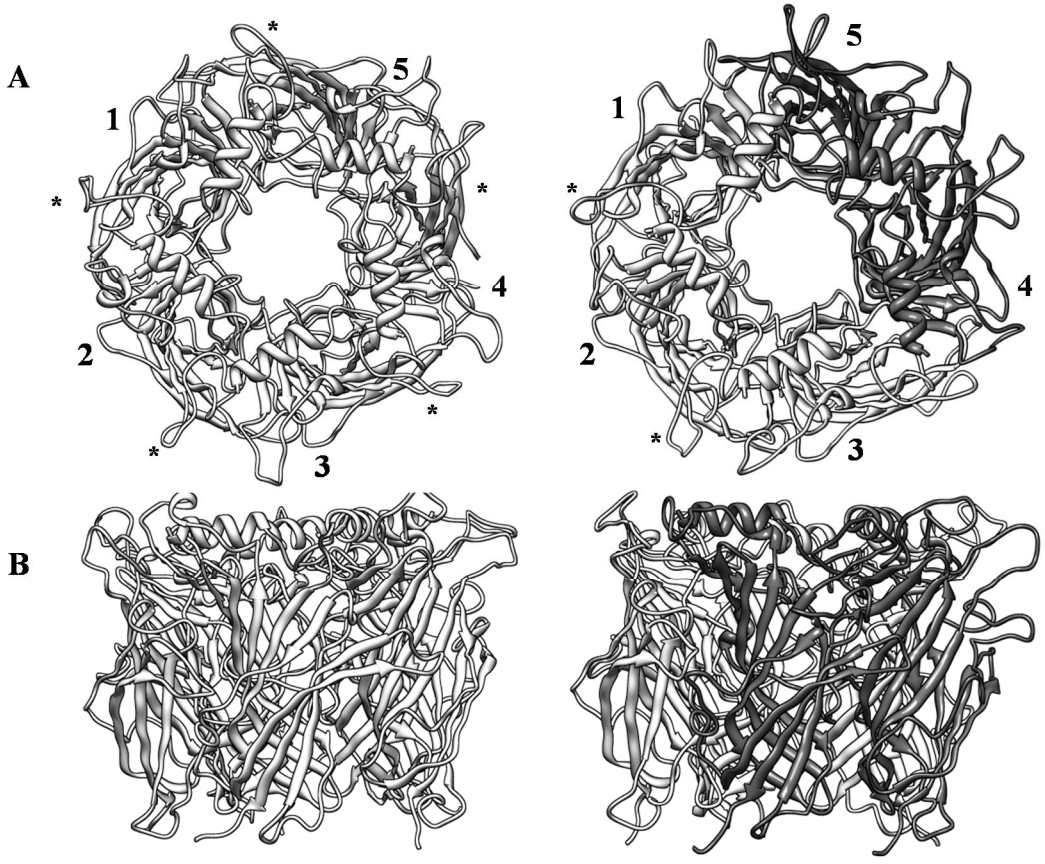

Figure 17. Homomeric and heteromeric Hco-UNC-49 pentameric receptors. A) Ariel view of homomeric and heteromeric Hco-UNC-49 pentameric receptors. . Each UNC-49 subunit is denoted by a corresponding number (1-5). Potential UNC-49B-B interface binding sites are denoted by an asterisk. Hco-UNC-49B subunits are highlighted in light grey. Hco-UNC-49C subunits are highlighted in dark grey B) Side view of homomeric and heteromeric Hco-UNC-49 pentameric receptors.

5.4 Future directions

Within this investigation, individual residues which play a key role in GABA sensitivity were identified via mutational analysis and two-electrode voltage clamp electrophysiology. This approach determined the effect of the various mutations on the macroscopic characteristics of the channel, such as the channel's EC_{50} (Wagner *et al.* 2004). Further analysis of the microscopic processes such as ligand binding-unbinding, channel opening-closing and channel desensitization-resensitization which may have contributed the changes in GABA sensitivity observed in this study (Colquhoun, 1998; Wagner *et al.* 2004) can be investigated using single-channel recordings and rapid ligand application (Wagner *et al.* 2004). However, based on previous research it appears as though the results associated with this study are caused by changes in GABA binding and not gating or channel activation (Sigel *et al.* 1992; Amin and Weiss, 1993; Boileau *et al.* 2002).

Homology modelling of both mutant and wild-type Hco-UNC-49 receptors indicate that it is highly plausible that Try^{166} (Loop B), Try^{218} (Loop C) or both interact with GABA via cationic-π interactions. One method to identify cation–π interactions is through the incorporation of fluorinated aromatics at prospective cation–π sites (Padgett *et al.* 2007). This method exploits the electrostatic properties of the cation–π binding affinity of aromatics by using the highly electronegative fluorine atom (Padgett *et al.* 2007). Fluorine's placement around the aromatic ring results in the diminished negative electrostatic potential on the face of the ring which in turn reduces the cation–π binding affinity of the residue (Padgett *et al.* 2007).

The exact role and function of Hco-UNC-49C in GABA binding in nematode

$GABA_A$ receptors has remained elusive. Despite its apparent contributions to channel pharmacology and desensitization kinetics, it appears that Hco-UNC-49C does not contribute directly to GABA binding. However, additional experiments would be required to confirm this hypothesis. Additionally, the receptor composition and potential arrangement of subunits within Hco-UNC-49 receptors has yet to be identified. Baur *et al.* (2006) has shown that mammalian $GABA_A$ receptors formed from a concatenated five subunit construct possessed comparable pharmacological properties to a corresponding non-concatenated $GABA_A$ receptor. Thus, a similar methodology with Hco-UNC-49 channels will allow the creation of perfectly defined receptor subunit composition and arrangement which may be useful in elucidating the function of Hco-UNC-49C.

The polymorphism Y166S is associated with a complete loss of GABA-activated responses in the homomeric channel. Interestingly, there are small responses within oocytes expressing Y166S mutant heteromeric channels at 25 mM GABA. Additionally, the equivalent mutation in mammalian $GABA_A$ receptors (Y157S) was also shown to respond to GABA albeit at very high concentrations of GABA (Amin and Weiss, 1993). Therefore, it is unclear whether the lack of GABA-evoked responses with the homomeric mutant is a result of defective channel assembly or trafficking of the channel to the membrane surface. To address these issues both radioligand-binding assays as well as Western blot analysis could be implemented to quantify the binding, if any, of GABA to the mutant channel and to identify whether the channel is expressed on the membrane surface, respectively.

5.5 Conclusion

The goal of this investigation was to identify which amino acids are essential for GABA sensitivity in the *H. contortus* UNC-49 GABA receptor. As a result, this thesis represents the first investigation of the molecular determinants important for the activation of an invertebrate $GABA_A$ receptor by its natural agonist. Therefore, this study has contributed an important step forward towards an increased understanding of the evolution of $GABA_A$ receptors.

Chapter 6 – References

Amin, J. and Weiss, D.S. 1993. $GABA_A$ receptor needs two homologous domains of the β subunit for activation by GABA but not pentobarbital. *Nature,* **366**:565-569

Bamber, B.A., Beg, A.A., Twyman, R.E. and Jorgensen, E.M. 1999. The *Caenorhabditis elegans unc-49* Locus Encodes Multiple Subunits of a Heteromultimeric GABA Receptor. *The Journal of Neuroscience,* **13**:348-5359

Bamber, B.A., Twyman, R.E. and Jorgensen, E.M. 2003. Pharmacological characterization of the homomeric and heteromeric UNC-49 GABA receptors in *C. elegans*. *British Journal of Pharmacology,* **138**: 883-893

Bamber, B.A., Richmond, J.E., Otto, J.F. and Jorgensen E.M. 2005. The composition of the GABA receptor at the *Caenorhabditis elegans* neuromuscular junction. *British Journal of Pharmacology*, **144**: 502–509

Bateson, A.N., Harvey, R.J., Bloks, C.C. and Darlison, M.G. 1990. Sequence of the chicken $GABA_A$ receptor beta 3-subunit cDNA. *Nucleic Acids Research,* **18**:5557

Baur, R., Minier, F. and Sigel, E. 2006. A $GABA_A$ receptor of defined subunit composition and positioning: Concatenation of five subunits. *FEBS Letters*, **580**:1616–1620

Blackhall, W.J., Prichard, R.K. and Beech, R.N. 2008. P-glycoprotein selection in strains of *Haemonchus contortus* resistant to benzimidazoles. *Veterinary Parasitology,* **152**:101–107

Blaxter, M. 2002. Molecular analysis of nematode evolution. *In Parasitic Nematodes. Molecular Biology, Biochemistry and Immunology* (ed. Kennedy, M. & Harnett, W.), pp. 1–25. CABI publishing, Oxford

Boileau, A.J., Newell, J.G. and Czajkowski, C. 2002. GABAA receptor *β*2 Tyr97 and Leu99 line the GABA-binding site: insights into mechanisms of agonist and antagonist actions. *Journal of Biological Chemistry*, **277**:2931–2937

Casida, J. E. 2009. Pest toxicology: The primary mechanisms of pesticide action. *Chemical Research in Toxicology,* **22**:609–619

Casida, J. E. 1993. Insecticide action at the GABA-gated chloride channel: Recognition, progress, and prospects. *Archives of Insect Biochemistry and Physiology,* **22**:13–23

Colquhoun, D. 1998. Binding, gating, affinity and efficacy: the interpretation of structure-activity relationships for agonists and of the effects of mutating receptors. *British Journal of Pharmacology,* **125**:924-947

Connolly, C.N. and Wafford, K.A. 2004. The Cys-loop superfamily of ligand-gated ion channels: the impact of receptor structure on function. *Biochemical Society Transactions,* **32**:529-534

Cromer, B.A., Morton, C.J. and Parker, M.W. 2002. Anxiety over GABAA receptor structure relieved by AChBP. *Trends in Biochemical Science,* **27**:280–287

Cully, D. F., Vassilatis, D. K., Liu, K. K., Paress, P. S., Van der Ploeg, L. H., Schaeffer, J. M. and Arena, J. P. 1994. Cloning of an avermectins sensitive glutamate gated chloride channel from Caenorhabditis elegans. *Nature,* **371**:707–711

Dent, J.A., Davis, M.W. and Avery, L. 1997. avr-15 encodes a chloride channel subunit that mediates inhibitory glutamatergic neurotransmission and ivermectin sensitivity in *Caenorhabditis elegans*. *EMBO Journal,* **16**:5867–79

Dorris, M., Viney, M.E. and Blaxter, M.L. 2002. Molecular phylogenetic analysis of the genus *Strongyloides* and related nematodes. *International Journal for Parasitology,* **32**:1507-1517

Ernst, M., Bruckner, S., Boresch, S. and Sieghart, W. 2005. Comparative Models of GABAA Receptor Extracellular and Transmembrane Domains: Important Insights in Pharmacology and Function. *Molecular Pharmacology,* **68**:1291–1300

Eswar, N., Madhusudhan, M.S., Marti-Renom, M.A. and Sali, A. 2005. BUILD_PROFILE: A module for calculating sequence profiles in MODELLER. http://www.salilab.org/modeller

Feng, X.P., Hayashi, J., Beech, R.N. and Prichard, R.K. 2002. Study of the nematode putative GABA type-A receptor subunits: evidence for modulation by ivermectin. *Journal of Neurochemistry,* **83**:870–878

ffrench-Constant, R. H., Mortlock, D. P., Shaffer, C. D., MacIntyre, R. J. and Roush, R. T. 1991. Molecular cloning and transformation of cyclodiene resistance in Drosophila: An invertebrate y-aminobutyric acid subtype A receptor locus. *Proceedings of the National academy of Sciences of the United States of America,* **88**:7209-7213.

Forrester, S.G., Prichard, R.K., Dent, J.A. and Beech, R.N. 2003. *Haemonchus contortus*: HcGluClaexpressed in *Xenopus* oocytes forms a glutamate-gated ion channel that is activated by ibotenate and the antiparasitic drug ivermectin. *Molecular and Biochemical Parasitology,* **129**:115-21

Gilleard, J.S. 2004. The use of *Caenorhabditis elegans* in parasitic nematode research. *Parasitology,* **128**:S49–S70

Gisselmann, G., Pusch, H., Hovemann, B.T. and Hatt, H. 2001. Two cDNAs coding for histamine-gated ion channels in *D. melanogaster*. *Nature Neuroscience,* **5**:11-12

Gurley, D., **Amin, J.**, **Ross, P.C.**, **Weiss, D.S. and White, G**. 1995. Point mutations in the M2 region of the alpha, beta, or gamma subunit of the $GABA_A$ channel that abolish block by picrotoxin. *Receptors Channels,* **3**:13–20

Harrison, N.J. and Lummis, S.C.R. 2006. Molecular modeling of the GABAC receptor ligand-binding domain. *Journal of Molecular Modeling,* **12**:317–324

Harvey, R.J., Vreugdenhil, E., Zaman, S.H., Bhandal, N.S., Usherwood, P.N., Barnard, E.A. and Darlison, M.G. 1991. Sequence of a functional invertebrate $GABA_A$ receptor subunit which can form a chimeric receptor with a vertebrate alpha subunit. *EMBO Journal,* **10**:3239-3245

Hevers, W. and Lüddens, H. 1998. The Diversity of $GABA_A$ Receptors: Pharmacological and Electrophysiological Properties of $GABA_A$ Channel Subtypes. *Molecular Neurobiology,* **18**:35-86

Holden-dye, L., Krogsgaard-Larsen, P., Nielsen, L. and Walker, R.J. 1989. GABA receptors on the somatic muscle cells of the parasitic nematode, Ascaris suum: stereoselectivity indicates similarity to a GABAA-type agonist recognition site. *British Journal of Pharmacology*, **98**:841-850

Hosie, A.M., Aronstein, K., Sattelle, D.B. and ffrench-Constant, R.H. 1997. Molecular biology of insect neuronal GABA receptors. *Trends in Neurosciences*, **20**:578-583

Hooft, R.W.W., Sander, C. and Vriend, G. 1997. Objectively judging the quality of a protein structure from a Ramachandran plot. *Computer Applications in the Biosciences,* **13**:425-430

Jin, Y., Hoskins, R. and Horvitz, H.R. 1994. Control of type-D GABAergic neuron differentiation by *C. elegans* UNC-30 homeodomain protein. *Nature*, **372**:780–783

Jin, Y., Jorgensen, E., Hartwieg, E. and Horvitz, H.R. 1999. The *Caenorhabditis elegans*gene unc-25 encodes glutamic acid decarboxylase and is required for synaptic transmission but not synaptic development. *Journal of Neuroscience*, **19**:539–548

Johnston. G.A.R. 1996. $GABA_A$ Receptor Pharmacology. *Pharmacology and Therapeutics,* **69**:173-198

Johnston, G.A.R. 2005. $GABA_A$ Receptor Channel Pharmacology. *Current Pharmaceutical Design,* **11:**1867-1885

Karlin, A. 2002. Emerging structure of the nicotinic acetylcholine receptors. *Nature Reviews Neuroscience,* **3**:102-114

Kash, T.L., Kim, T., Trudell, J.R. and Harrison, N.L. 2004. Evaluation of a proposed mechanism of ligand-gated ion channel activation in the $GABA_A$ and glycine receptors. *Neuroscience Letters,* **371**:230–234

Kwa, M. S., Veenstra, J. G., Van Dijk, M. and Roos, M. H. 1995. Beta-tubulin genes from the parasitic nematode *Haemonchus contortus* modulate drug resistance in *Caenorhabditis elegans*. *Journal of Molecular Biology,* **246**:500–510

Laskowski, R.A, Rullmann, J.A, MacArthur, M.W, Kaptein, R, and Thornton, J.M. 1996. AQUA and PROCHECK NMR: programs for checking the quality of protein structures solved by NMR. *Journal of Bimolecular NMR*, **8**:477–486

Laughton, D.L., Amar, M., Thomas, P., Towner, P., Harris, P., Lunt, G.G., and Wolstenholme, A.J. 1994. Cloning of a putative inhibitory amino acid receptor subunit from the parasitic nematode *Haemonchus contortus*. *Receptors and Channels,* **2**:1555-1563

Lolait, S.J., O'Carroll, A., Kusano, K., Muller, J., Brownstein, M.J. and Mahan, L.C. 1989. Cloning and expression of a novel rat $GABA_A$ receptor. *FEBS Letters,* **246**:145-148

Lee, D., Su, H. and O'Dowd, D.K. 2003. GABA Receptors Containing Rdl Subunits Mediate Fast Inhibitory Synaptic Transmission in *Drosophila* Neurons. *The Journal of Neuroscience,* **23**:4625– 4634

Lester, H.A., Dibas, M.I., Dahan, D.S., Leite, J.F. and Dougherty, D.A. 2004. Cys-loop receptors: new twists and turns. *TRENDS IN Neuroscience,* **27**:329-336

Lovell, S. C., Davis, I. W., Arendall, W. B., III, de Bakker, P. I., Word, J. M., Prisant, M. G., Richardson, J. S., and Richardson, D. C. 2003. Structure validation by Cα geometry: φ, ψ, and Cβ deviation. *Proteins,* **50**:437–450

Lummis, S.C.R. 2009. Locating GABA in GABA receptor binding sites. *Biochemical Society Transactions,* **37**:1343–1346

Martin, R.J. 1993. Neuromuscular transmission in nematode parasites and antinematodal drug action. *Pharmacology and Therapeutics*, **58**:13-50.

McGonigle, I. and Lummis, S.C.R. 2010. Molecular Characterization of Agonists That Bind to an Insect GABA Receptor. *Biochemistry*, **49**:2897–2902

McKernan, R.M. and Whiting, P.J. 1996. Which $GABA_A$ receptor subtypes really occur in the brain? *Trends in Neuroscience,* **19**:139 –143

McIntire, S.L., Jorgensen, E., Kaplan, J. and Horvitz, H.R. 1993a. The GABAergic nervous system of *Caenorhabditis elegans*. *Nature,* **364**:337–341

McIntire, S.L., Jorgensen, E. and Horvitz, H.R. 1993b. Genes required for GABA function in *Caenorhabditis elegans*. *Nature,* **364**:334–337

Mes, T.H.M. 2004. Purifying Selection and Demographic Expansion Affect Sequence Diversity of the Ligand-Binding Domain of a Glutamate-Gated Chloride Channel Gene of *Haemonchus placei*. *Journal of Molecular Evolution,* **58**:466–478

Miller, P.S. and Smart, T.G. 2010. Binding, activation and modulation of Cys-loop receptors. *Trends in Pharmacological Sciences*, **31**:161-174

Murzin, A.G. 1998. How far divergent evolution goes in proteins. *Current Opinion in Structural Biology,* **8**:380-387

Newell, J.G. and Czajkowski, C. 2003. The GABAA receptor α1 subunit Pro174–Asp191 segment is involved in GABA binding and channel gating. *Journal Biological Chemistry*, **278**:13166–13172

Newton, S.E. and Meeusen, E.N.T. 2003. Progress and New Technologies for Developing Vaccines Against Gastrointestinal Nematode Parasites of Sheep. *Parasite Immunology,* **25**:283-296

Nikolaou, S. and Gasser, R.B. 2006. Prospects for Exploring Molecular Developmental Processes in *Haemonchus contortus*. *International Journal for Parasitology,* **36**:859-868

Njue, A.I. and Prichard, R.K. 2004. Genetic variability of glutamate-gated chloride channel genes in ivermectin-susceptible and -resistant strains of *Cooperia oncophora*. *Parasitology,* **129**:741–751

Parkinson, J., Mitreva, M., Whitton, C., Thomson, M., Daub, J., Martin, J., Schmid, R., Hall, N., Barrell, B., Waterston, R.H., McCarter, J.P. and Blaxter, M.L. 2004. A transcriptomic analysis of the phylum Nematoda. *Nature Genetics*, **36**:1259-1267

Padgett, C.L., Hanek, A.P., Lester, H.A.. Dougherty, D.A., and Lummis, S.C.R. 2007. Unnatural Amino Acid Mutagenesis of the GABAA Receptor Binding Site Residues Reveals a Novel Cation–π Interaction between GABA and β2Tyr97. *The Journal of Neuroscience*, **27**:886–892

Pettersen, E.F., Goddard, T.D., Huang, C.C., Couch, G.S., Greenblatt, D.M., Meng, E.C. Ferrin, T.E. 2004. UCSF Chimera—a visualization system for exploratory research and analysis. *Journal of Computational Chemistry*, **25**:1605–1612.

Pirri, J.K., McPherson, A.D., Donnelly, J.L., Francis, M.M. and Alkema, M.J. 2009. A tyramine-gated chloride channel coordinates distinct motor programs of a *Ceanorhabditis elegans* escape response. *Neuron,* **62**:526-538

Pless, S.A., Millen, K.S., Hanek, A.P., Lynch, J.W., Lester, H.A., Lummis, S.C.R. and Dougherty, D.A. 2008. A cation-p interaction in the binding site of the glycine receptor is mediated by a phenylalanine residue. *The Journal of Neuroscience*, **28**:10937–10942

Rao, V.T.S, Siddiqui, S.Z., Prichard, R.K. and Forrester, S.G. 2009. A dopamine-gated ion channel (HcGGR3*) from *Haemonchus contortus* is expressed in the cervical papillae and is associated with macrocyclic lactone resistance. *Molecular and Biochemical Parasitology*, **166**:54-61

Sali, A. and Blundell, T.L. 1993. Comparative protein modelling by satisfaction of spatial restraints. *Journal of Molecular Biology*, **234**:779–815.

Schofield, P.R., Darlison, M.G., Fujita, N., Burt, D.R., Stephenson, F.A., Rodriguez, H., Rhee, L. M., Ramachandran, J., Reale, V., Glencorse, T.A., Seeburg, P.H. and Barnard, E.A. 1987. Sequence and functional expression of the $GABA_A$ receptor shows a ligand-gated receptor super-family. *Nature*, **328**:221-227

Schuske, K., Beg, A. A. and Jorgensen, E. M. 2004. The GABA nervous system in *C. elegans*. *TRENDS in Neurosciences*, **27**:407-414

Siddiqui, S.Z., Brown, D.D.R, Rao, V.T.S. and Forrester, S.G. 2010. An UNC-49 GABA receptor subunit from the parasitic nematode Haemonchus contortus is associated with enhanced GABA sensitivity in nematode heteromeric channels. *Journal of Neurochemistry*, **5**:1113-1122

Sigel, E., Baur, R., Kellenberger, S. and Malherbe, P. 1992. Point mutations affecting antagonist affinity and agonist dependent gating of GABAA receptor channels. *EMBO Journal* **11**: 2017–2023

Sixma, T. K. and Smit, A. B. 2003. Acetylcholine binding protein (AChBP): A secreted glial protein that provides a high-resolution model for the extracellular domain of pentameric ligand-gated ion channels. *Annual Review of Biophysics and Biomolecular Structure*, **32**:311–334

Skinner, T.M., Bascal, Z.A., Holden-Dye, L., Lunt, G.G., and Wolstenholme, A.J. 1998. Immunocytochemical localization of a putative inhibitory amino acid receptor subunit in the parasitic nematodes *Haemonchus contortus* and *Ascaris suum*. *Parasitology*, **117:**89-96

Smith, G.B. and Olsen, R.W. 1994. Identification of a [3H]muscimol photoaffinity substrate in the bovine γ -aminobutyric acidA receptor α subunit. *Journal of Biological Chemistry*, **269**:20380–20387

Strange, K. 2006. An overview of C. elegans biology. *Methods in Molecular Biology*, **351**:1-11

Thompson, A.J. and Lummis, S.C.R. 2007. The 5-HT3 receptor as a therapeutic target. *Expert Opinion* on Therapeutic *Targets*, 11:527-540

Wagner, D.A. and Czajowski, C.2001. Structure and dynamics of the GABA binding pocket: A narrowing cleft that constricts during activation. *The Journal of Neuroscience*, **21**:67-74

Wagner, D.A., Czajowski, C. and Jones, M.V. 2004. An arginine involved in GABA binding an unbinding but not gating of the GABAA receptor. *The Journal of Neuroscience*, **24**:2733-2741

Walker, R.J., Colquhoun, L. and Holden-Dye, L. 1992. Pharmacological profiles of the GABA and acetylcholine receptors from the nematode, Ascaris suum. *Acta Biologica Hungarica*, **43**:59-68

Weiss, J.N. 1997. The Hill equation revisited: uses and misuses. *The FASEB Journal*, **11**:835-841

Westh-Hansen, S.E., Witt, M.R., Dekermendjian, K., Liljefors, T., Rasmussen, P.B. and Nielsen, M. 1999. Arginine residue 120 of the human GABAA receptor α1 subunit is essential for GABA binding and chloride ion current gating. *NeuroReport*, **10**:2417–2421

Yates, D.M., Portillo, V. and Wolstenholme, A.J. 2003. The avermectin receptors of *Haemonchus contortus* and *Caenorhabditis elegans*. *International Journal for Parasitology*, **33**:1183–1193

Ymer, S., Schofield, P.R., Draguhn, A., Werner, P., Kohler, M. and Seeburg, P.H. 1989. $GABA_A$ receptor beta subunit heterogeneity: functional expression of cloned cDNAs. *EMBO Journal*, **8**:1665-1670

Chapter 7 – Appendices

Appendix A – Mutation Primers

Table A1: Designed primers for Hco-UNC-49-*C. elegans* associated mutation introduction

Mutation	Forward Primer (5' - 3')	Reverse Primer (3' - 5') Antisense
T169E (UNC-49B)* (54 base pairs) 80.15 °C Tm	CGATGCAAGCTGGAAATTGAAAGC TATGGCTATGAGATGGCTGATATC GACTAC	GTAGTCGATATCAGCCATCTCATA GCCATAGCTTTCAATTTCCAGCTTG CATCG
M170T (UNC-49B)* (42 base pairs) 78.67 °C Tm	TGGAAATTGAAAGCTATGGCTATA CAACGGCTGATATCGACT	AGTCGATATCAGCCGTTGTATAGC CATAGCTTTCAATTTCCA
M170S (UNC-49B)* (48 base pairs) 79.50 °C Tm	GAAATTGAAAGCTATGGCTATACA AGCGCTGATATCGACTACTTCTGG	CCAGAAGTAGTCGATATCAGCGCT TGTATAGCCATAGCTTTCAATTTC
A171K (UNC-49B)* 49 (base pairs) 78.34 °C Tm	TTGAAAGCTATGGCTATACAATGA AGGATATCGACTACTTCTGGGGAC G	CGTCCCCAGAAGTAGTCGATATCC TTCATTGTATAGCCATAGCTTTCAA
S217K (UNC-49B)* (44 base pairs) 78.39 °C Tm	CAAGCAACCACATCATCAGGGAAG TATAGGCGTTTATACTTTGA	TCAAAGTATAAACGCCTATACTTCC CTGATGATGTGGTTGCTTG
G167A (UNC-49C)** (36 base pairs) 78.19 °C Tm	TCGAAATTGAAAGCTATGCTTATTC CACGGCAGCCA	TGGCTGCCGTGGAATAAGCATAGC TTTCAATTTCGA
A214S (UNC-49C)** (36 base pairs) 79.97 °C Tm	GGACAATGGCCACTACCAGTTCAG GCTCCTATTCCC	GGGAATAGGAGCCTGAACTGGTAG TGGCCATTGTCC
S217T (UNC-49C)** (29 base pairs) 78.81 °C Tm	CTACCGCTTCAGGCACCTATTCCCG ACTC	GAGTCGGGAATAGGTGCCTGAAGC GGTAG

***All mutation positions are located in the coding sequence of the Hco-UNC-49B protein**
**** All Mutation positions are located in the coding sequence of the Hco-UNC-49C protein**

Table A2: Designed primers for Hco-UNC-49B- $GABA_A$ β_2 subunit associated mutation introduction

Mutation*	Forward Primer (5' - 3')	Reverse Primer (3' - 5') Antisense
Y166S (48 base pairs) 78.52 °C Tm	GATGCAAGCTGGAAATTGAAAGCA GTTGCTATACAATGGCTGATATCG	CGATATCAGCCATTGTATAGCAAC TGCTTTCAATTTCCAGCTTGCATC
Y166F (40 base pairs) 79.55 °C Tm	CGATGCAAGCTGGAAATTGAAAGC TTTGGCTATACAATGG	CCATTGTATAGCCAAAGCTTTCAAT TTCCAGCTTGCATCG
T169S (43 base pairs) 78.73 °C Tm	GAAATTGAAAGCTATGGCTATTCA ATGGCTGATATCGACTACT	AGTAGTCGATATCAGCCATTGAAT AGCCATAGCTTTCAATTTC
S215T (40 base pairs) 79.10 °C Tm	ATTACACACAAGCAACCACATCAA CGGGGTCGTATAGGCG	CGCCTATACGACCCCGTTGATGTG GTTGCTTGTGTGTAAT
Y218F (37 base pairs) 78.28 °C Tm	CCACATCATCAGGGTCGTTTAGGC GTTTATACTTTGA	TCAAAGTATAAACGCCTAAACGAC CCTGATGATGTGG

***All mutation positions are located in the coding sequence of the Hco-UNC-49B protein**

Table A3: Designed primers for Hco-UNC-49C- $GABA_A$ β_2 subunit associated mutation introduction

Mutation*	Forward Primer (5' - 3')	Reverse Primer (3' - 5') Antisense
Y166F (36 base pairs) 78.19 °C Tm	GCAAGCTCGAAATTGAAAGCTTTGGTTATTCCACGG	CCGTGGAATAACCAAAGCTTTCAATTTCGAGCTTGC
S215T (33 base pairs) 78.59 °C Tm	CAATGGCCACTACCGCTACGGGCTCCTATTCCC	GGGAATAGGAGCCCGTAGCGGTAGTGGCCATTG
Y218F (29 base pairs) 80.22 °C Tm	CGCTTCAGGCTCCTTTTCCCGACTCCTGC	GCAGGAGTCGGGAAAAGGAGCCTGAAGCG

***All mutation positions are located in the coding sequence of the Hco-UNC-49C protein**

Table A4: Designed primers for Hco-UNC-49- $GABA_A$ α_1 subunit associated mutation introduction

Mutation*	Forward Primer (5' - 3')**	Reverse Primer (3' - 5') Antisense**
F63L (44 base pairs) 78.80 °C Tm	ATATGGACTTTACGCTAGATTTATA TATGCGACAAACATGGCAG	CTGCCATGTTTGTCGCATATATAAA TCTAGCGTAAAGTCCATAT
Y64L (47 base pairs) 80. 33 °C Tm	GGATATGGACTTTACGCTAGATTT CTTAATGCGACAAACATGGCAGG	CCTGCCATGTTTGTCGCATTAAGAA ATCTAGCGTAAAGTCCATATCC
M65L (42 base pairs) 78.67 °C Tm	GATATGGACTTTACGCTAGATTTC TATTTGCGACAAACATGG	CCATGTTTGTCGCAAATAGAAATCT AGCGTAAAGTCCATATC

***All mutation positions are located in the coding sequence of the Hco-UNC-49 subunit proteins**
**** Primers were designed for complementation to both Hco-UNC-49 subunit nucleotide sequences**